USING REAL-TIME PCR TO EXAMINE RETINOIC ACID PATHWAY GENE EXPRESSION DURING EARLY ZEBRAFISH DEVELOPMENT

By

SHARON ELIZABETH NORTON

A THESIS PRESENTED TO THE GRADUATE SCHOOL
OF THE UNIVERSITY OF FLORIDA IN PARTIAL FULFILLMENT
OF THE REQUIREMENTS FOR THE DEGREE OF
MASTER OF SCIENCE

UNIVERSITY OF FLORIDA

2009

To my husband Michael and my son Nicholas

ACKNOWLEDGMENTS

I would like to thank my chair, Dr. Peter McGuire, whose advice and guidance was always delivered at the right time, in the right amount and in the right place which was essential for the proper development of this thesis. His patience and willingness to work with a full-time-employed-over-the-traditional-age student was truly a gift that was very much appreciated. Dr. McGuire is a wonderful teacher and his recent retirement from the University of Florida Department of Biochemistry and Molecular Biology is surely a loss for them. I also thank the other members of my advisory committee, Dr. David Barber and Dr. Gregory Schultz, for their input, guidance and support. Thanks go out to my staff at the Interdisciplinary Center for Biotechnology Research (ICBR), David Nolan and James Pennington, for their patience, assistance and excellent work in the laboratory to help keep the ICBR Education and Training Laboratory running smoothly when I was absent to attend classes toward the completion of this degree. Last but not least, I thank my husband Michael and my son Nicholas for being supportive, flexible and filling in the gaps when I needed to be away from the family to complete homework and laboratory research.

TABLE OF CONTENTS

page

LIST OF TABLES

LIST OF FIGURES

Abstract of Thesis Presented to the Graduate School
of the University of Florida in Partial Fulfillment of the
Requirements for the Degree of Master of Science

USING REAL-TIME PCR TO EXAMINE RETINOIC ACID PATHWAY GENE EXPRESSION DURING EARLY ZEBRAFISH DEVELOPMENT

By

Sharon Elizabeth Norton

May 2009

Chair: Peter McGuire
Major: Medical Science

Real-time PCR, fluorescence based detection of amplification products through the use of a DNA-binding dye or probe chemistry, has become a useful tool to quantify differences in mRNA expression. This technique is especially beneficial when the availability of mRNA's is very low such as in small amounts of tissue, primary cells or cells obtained by laser capture micro-dissection. Based on this knowledge, can real-time PCR be used to quantify changes in mRNA expression during early development of zebrafish?

Retinoic acid (RA) and its derivatives have a profound effect on vertebrate development. An excessive or insufficient amount at specific times during development causes defects. The pathway of metabolites between the uptake of vitamin A (retinol) from the yolk and later from the diet, conversion to retinoic acid and production of degradation products, is in a tightly regulated balance during early development. Zebrafish embryos were collected at early time intervals based on hours post fertilization (hpf) and high quality total RNA was extracted. To determine which messages in the RA pathway are having the greatest fold change normalized to an endogenous control and relative to the other time points during early development, a panel of twelve different polymerase chain reaction (PCR) primer sets was designed, optimized and used to screen zebrafish RNA at several time points using both SYBR® Green chemistry and real-time

PCR. The most dramatic fold changes were observed in retinaldehyde dehydrogenase 2 (RALDH2), retinoic acid receptor gamma (RARG) and cytochrome P450 26B1 (CYP 26B1). To validate their change in expression and confirm the SYBR® Green real-time PCR data, pre-designed TaqMan® primers and probes were used to construct a standard curve and perform absolute quantification. To date the method more commonly used to determine the relative amount and location within zebrafish embryos has been *in situ* hybridization. The practical advantage of real-time PCR is that it requires less time, lower cost, and less training to master technically. Additionally, an exact copy number can be obtained with real-time PCR which is not possible with *in situ* hybridization. Results with these three retinoic acid pathway mRNAs, where expression increases dramatically between 5hpf and 24 hpf, show that this screening panel can be used effectively to monitor quantitatively components of the RA pathway during early development.

In order to fulfill the work requirements for my position as Education Coordinator at the Interdisciplinary Center for Biotechnology Research (ICBR) Education and Training Core Laboratory while simultaneously completing this thesis, the knowledge gained from this research was written as a hands-on training exercise in real-time PCR for graduate level courses. The experiment was designed to fit with the overall theme of carbonic anhydase, relay the basics of real-time PCR and be feasible logistically in a classroom of fifty-two graduate level students while adhering to a timed schedule. Additionally, a bioinformatics exercise using their real-time PCR data and relative expression software tool (REST) was included to maintain the continuity of the concurrent bioinformatics training.

CHAPTER 1
INTRODUCTION

The Physiological Effects Of Vitamin A

Vitamin A plays an important functional role in vertebrates for vision, gene regulation, immunity, red blood cell production, nutrient interactions, and growth and development. Excess or insufficient amounts of vitamin A during development can create severe teratogenic effects. Deficiencies of vitamin A in mature organisms can lead to a number of infectious diseases, osteoporosis or blindness. Vitamin A in the form of retinol or the provitamin A β-carotene must be converted to retinaldehyde and then retinoic acid by specific enzymes to be in a usable form for the organism. Understanding how the various metabolites of the retinoic acid pathway change and are regulated during early development will provide information about what levels are at the proper places, times and concentrations. In this thesis a screening panel of ten genes of interest in the retinoic acid (RA) pathway, two primer sets for endogenous controls and real-time PCR are used to observe and quantify those gene expression changes at different time points of early development in zebrafish.

Vitamin A is taken up in the diet usually from plant sources as the provitamin β-carotene, a carotenoid. Plant carotenoids, orange-yellow in color, are similar to chlorophyll in that they harvest photons for photosynthesis. Other examples of carotenoids in plants are alpha-carotene and beta-cryptoxanthin which are also converted to vitamin A but not as efficiently as β-carotene. Vitamin A is also available in the fat of plant-eating animals where it is called preformed vitamin A and when subsequently absorbed in the diet is in the form of retinol. Once β-carotene is cleaved enzymatically in the small intestine, two molecules of all-*trans* retinal are formed and reversibly converted to all-*trans* retinol which is stored in the liver or circulated in the blood while bound to a retinol-binding protein (RBP). The transition between all-*trans*-

retinol and 11-*cis*-retinal in the phototransduction and visual cycle ultimately leads to the release of neurotransmitters by photoreceptor cells and facilitates vision[1]. When the visual cycle progresses into the rod outer segment, 11-*cis*-retinal binds to opsin to become rhodopsin. When the rhodopsin absorbs light, 11-*cis*-retinal is converted to all-*trans*-retinal and Rho* is released as an active photoproduct. This conformational change induces a calcium ion channel which the brain recognizes as light. The all-*trans*-retinal is reduced by retinol dehydrogenase to all-*trans*-retinol by reduced nicotinamide adenine dinucleotide phosphate (NADPH); the all-*trans*-retinol then leaves the rod outer segment, crosses over the subretinal space and into the retinal pigment epithelium (RPE). In the RPE the all-*trans*-retinol is esterified to all-*trans*-retinyl ester, and then converted to free fatty acid and 11-*cis*-retinol by isomerohydrolase. 11-*cis*-retinol is then converted to 11-*cis*-retinal which again to binds opsin to repeat the visual cycle. The general outline of the regeneration cycle was depicted in a paper in *Nature* as far back as 1934[2] (Figure 1-1).

Vitamin A deficiency (VAD) can lead to inadequate retinol being available to the retina, resulting in an impaired dark adaptation of the eyes and night blindness. VAD is the leading cause of preventable blindness in developing countries[3]. The connections between VAD and ocular problems were noticed very early after the vitamin's discovery in 1917. As VAD becomes more severe there is a progression of reversible ailments that can occur. After night blindness, a loss of goblet cells can lead to dry eyes, and dead epithelial and microbial cell accumulation form Bitot's spots and corneal xerosis. The xerosis leads to ulceration of the cornea which is not a reversible condition. Prior to ulceration, the above ailments can be rescued by increased vitamin A intake and RA production[4]. Vitamin A is clearly an important component of healthy eyes and vision.

Retinoic acid has an important role in gene expression. This active metabolite of vitamin A activates retinoid receptors that potentially regulate other genes. Where the 11-*cis*-retinoids were important in vision, all-*trans*-retinoic acid and 9-*cis* retinoic acid have major roles in other biological processes (Figure 1-2). All-*trans*-RA binds with high affinity to retinoic acid receptors RARα, RARβ and RARγ. The 9-cis-RA can also bind to these receptors but is widely believed to bind with higher affinity to the retinoic X receptor family known as RXRα, β, and γ[5]. When RAR and RXR proteins combine into heterodimers under physiological conditions, they are capable of binding to DNA at specific sequences that are commonly located in a regulatory region of a gene. These sequences are called retinoic acid response elements (RARE) and transport to the DNA in the nucleus of the cell occurs while bound to cytoplasmic retinoic acid-binding proteins (CRABP). In the absence of ligand the heterodimer remains bound at the RARE region associated with a co-repressor to induce transcriptional silencing by deacetylating histones thereby increasing chromatin condensation. One of the targets for RAR/RXR heterodimers is the *Hox* genes which encode important transcription factors for genes expressed during embryogenesis. RXR can also bind and form heterodimers with thyroid hormone receptors or vitamin D receptors which give them an even larger range of potential genes to affect (Figure 1-3). Since the potential exists for the RA to affect a large number of different genes regulating many different biological processes, the metabolites in this pathway should be very specifically controlled. In addition to transcriptional regulation it is proposed that autoregulation may also be at work to maintain the correct levels of retinoic acid. This theory was proposed because the initiation of the degradation of some retinoid receptor proteins is sometimes retinoid dependent[6]. Examples that may be important in autoregulation are lecithin:retinol acyltransferase (LRAT) and a cytochrome P450, CYP 26. LRAT catalyzes

esterification of retinol in small intestine, liver, retina, skin, testis and lung. CYP26 is expressed in numerous embryonic and adult tissues. All-*trans*-RA induces the CYP26 gene and is also the substrate of the CYP26 protein, making it a likely candidate for autoregulation. Retinoic acid metabolism that is not properly regulated in a biological system, either transcriptionally or through autoregulatory processes, could have severe consequences on gene expression.

It was observed early on that vitamin A deficient animals were more likely to be adversely affected by infections than animals that were not deficient[7]. The anti-infective attributes of RA arise from its ability to stimulate and/or regulate the immune system. Important components of the innate and adaptive immune responses are modulated by RA, including dendritic cell maturation, cytokine production, T and B cell activation, antibody responses and mucosal immunity. This active metabolite has also been shown to enhance thymocyte differentiation and activation by mitogens[8]. T cells exposed to subnanomolar concentrations of RA induce gut-homing receptors and migration to the small intestine while at the same time suppressing the expression of skin-homing molecules. If memory cells that have already committed to a skin-homing phenotype could actually be reprogrammed by exposure to RA, this treatment could have positive therapeutic impact and possibly explain why retinoids are helpful in T cell-mediated cutaneous autoimmune diseases like psoriasis[9]. Interestingly, when RA is mixed with polyriboinosinic: polyribocytidylic acid (PIC), a synthetic immunity booster, the immune response to a tetanus shot is highly elevated. Receiving vitamin A through nutrition may play an important role in regulating immunity by giving nutritional-immunological assistance during vaccination[10]. The body strictly controls how much retinoic acid is made from ingested vitamin A to ensure that levels do not exceed what is needed. As our understanding of the immune system expands perhaps RA will be discovered to have even more therapeutic roles.

RA has an impact on the differentiation of hematopoietic cells and pancreatic endocrine progenitor cells. When bone marrow was studied from vitamin A deficient animals, a decrease in hematopoietic cells was found. Growth of normal human early erythroid progenitors *in vitro* was enhanced with the addition of retinoic acid. In contrast RA was found to have anti-leukemic effects *in vitro* and to inhibit clonal growth of myeloid leukemia cells[11]. RA receptor signaling was required in early pancreatic progenitor cells during development by promoting the generation of $Ngn3^+$ endocrine progenitor cells which are further differentiated into β-cells. RALDH1, an RA–synthesizing enzyme, is expressed when β-cells are being generated in embryonic mouse and human pancreas[12].

RA is important in a number of body systems including bone structure and function. Its precursor, vitamin A, has been administered to control acne and psoriasis, but bone lesions, arthritis, myopathy and vasculitus have been reported when levels were too high. Mice that were deficient in CYP26A1, which metabolizes retinol into hydroxylated and oxidized derivatives, were found to have lethal phenotypic changes similar to those produced by excess administration of vitamin A. It was suggested that perhaps abnormalities in the retinol pathways could be associated with ankylosing spondylitis, a disease characterized by pathological bone formation, but the exact effect of retinol on the bone remains unresolved in that study[13]. RA clearly plays an important if not yet fully understood role in cell differentiation and erythrocyte production.

Interactions between RA and other nutrients like zinc and iron are important considerations when discerning the effect on animal health or retinoic acid homeostasis. Zinc is involved with absorption, mobilization, transport and metabolism of vitamin A. There is some evidence that vitamin A in turn affects zinc absorption and utilization. There are two different proposed mechanisms to explain the dependence of vitamin A on zinc. The first states that zinc deficiency

may lead to decreased retinol-binding protein (RBP) in the liver which means that there will be less RBP in the plasma. The other mechanism proposes that the conversion of retinol to retinal by retinol dehydrogenase is zinc dependent[14]. The exact effect of zinc deficiency on vitamin A remains unclear.

Anemia as a result of iron deficiency has similarities to vitamin A deficiencies to which growing children and women of reproductive age are the most vulnerable. It is suggested that vitamin A and iron affect each other metabolically thereby altering the other's nutritional status. In a study of young male Sprague-Dawley rats that displayed moderate iron deficiency anemia, RA was still able to accumulate in the liver while the serum retinol was decreased indicating that a decrease in iron may affect the irreversible utilization and absorption of vitamin A[15]. In a study of children that had anemia and were treated with RA, it was determined that the serum retinol was decreased while it was not in the placebo treated children[16]. These studies indicate that lower plasma retinol as a result of decreased iron coincided with increased liver vitamin A, suggesting that these nutrients may be affecting each other. Nutrients taken up through diet must be considered when investigating the effects of RA on the biological system.

The effects of retinoic acid on early development are profound. Vertebrate development requires RA[17], but when not available at the right time or in the wrong amount, RA becomes a potent teratogen[18]. RA has important roles in the nervous system and anterior posterior patterning. Most of its effects on development are a result of RA's ability to regulate gene expression. Retinoic acid response elements (RAREs) and the retinoid X receptors have conserved sequences among species. They work together to activate RA responsive promoters. Specific isoforms have been found for retinoid signal transduction in embryos and adults. If mutations are made to these isoforms, the effects are lethal. It is thought that each retinoic acid

receptor has at least one unique function which could explain why its sequence is conserved across vertebrates. An important function of RA that affects embryonic development is its regulation of homeobox genes that are transcription factors. For example, an RA gradient may directly control Hox-d, which affects polarization activities in the limb. Due to the potential developmental defects if RA is absent or in excess, the enzymes that both produce and degrade it keep the RA signaling and amounts in an appropriate balance[19].

Retinoic Acid Pathway And Experimental Plan

To create our screening system for real-time PCR, important expressed messages in zebrafish along the retinoic acid pathway from retinol to degradation products were chosen. First is the reversible process when retinol is converted to retinaldehyde by alcohol dehydrogenases ADH5, ADH8A and ADH8B. The ADH5 gene encodes glutathione-dependent formaldehyde dehydrogenase also known as a class III alcohol dehydrogenase chi subunit. Other substrates for this enzyme besides retinol are ethanol, aliphatic alcohols, hydroxysteroids and lipid peroxidation products. It is important in cellular metabolism for the elimination of formaldehyde[20]. Both ADH8a and ADH8b have been genetically mapped to chromosome 13 of the zebrafish. There is a 72% homology of the ADH8a and 66% homology ADH8b of zebrafish to the human ADH1B2. A study of these two zebrafish dehydogenases shows that ADH8A metabolizes ethanol but ADH8B does not. They both failed to metabolize methanol. Expression studies on the ADH8A and ADH8B show that they are both developmentally expressed as early as 24 hpf and were found also in adult zebrafish tissues[21].

The next enzyme is β-carotene cyclooxygenase (BCOX) which irreversibly converts β-carotene (provitamin A) to retinaldehyde. Retinaldehyde can exist in two forms, 11-*cis* retinal and all-*trans* retinal. The straightening of the molecule to the all-*trans* configuration occurs in

response to a photon of light. When light is removed, the molecule relaxes back to its more stable form.

Retinaldehyde is oxidized to retinoic acid by retinaldehyde dehydrogenase (RALDH2). Studies that knock out the expression of RALDH2 activity in vivo display a VAD phenotype. The patterning of the intestine also appears to depend on the RALDHs[22]. Another study that focused on knock out of the RALDH2 in mouse embryo found that its activity is crucial for proper RA production within the embryonic trunk; knock out results in early embryonic lethality[23] and exhibits defective morphogenesis of various forebrain derivatives[24].

After retinaldehyde is oxidized to retinoic acid by RALDH2, RA subsequently binds to a subset of nuclear hormone receptors which affect gene function. The retinoic acid receptors RARAA, RARAB and RARG were investigated. Each isoform has several splice variants. When the RA-bound retinoic acid receptor (RAR) binds with a retinoid X receptor, the complex is then able to bind to retinoic acid response elements of DNA and change gene expression.

Finally on the retinoic pathway we explore two degradation product enzymes: Cytochrome P450, family 26, subfamily A, polypeptide 1 (CYP26A1) and cytochrome P450, family 26, subfamily B, polypeptide 1 (CYP26B1). The CYP superfamilies are made up of monooxygenases that catalyze many biological reactions. They are generally expressed in the liver but have also been located in the kidney, lung, gut mucosa, placenta, reproductive organs, embryonic tissues and the brain[25]. These enzymes act on all-*trans*-retinoic acid to regulate the cellular levels of RA thereby having an impact on gene regulation in adult and embryonic tissues. CYP 26A1 has both 4-hydroxylation and 18-hydroxylation activities and CYP26B1 is involved with specific inactivation of all-trans-retinoic acid to hydroxylated forms[26]. (Figure 1-4)

RA is a biologically relevant biomarker for zebrafish development. Biomarkers are specific traits that can be objectively measured to indicate normal biological processes. They are highly useful in the early detection of drug dosage levels, in vitro studies in tissue samples, in vivo studies in animal models and early phase clinical trials for helping to determine "proof of concept." One of the earliest examples of an effective vaccine biomarker is the polio antibody neutralization assay that is still in use today[27]. Using a panel of real-time PCR SYBR® Green primers to important components in the retinoic acid pathway will quickly detect if one is shifted from its normal level of expression. This system may potentially be useful for detection of anthropogenic or natural biological toxins in our environment that would have detrimental effects on embryological development.

In the studies described in this thesis I will characterize the retinoic acid pathway using real-time PCR and develop a graduate student training experiment using the information and experience gained during this research, in four main sections:

1) Harvest embryos at time points in early embryogenesis and extract total RNA that is verified for quality and quantity.

2) Design and optimize 12 different primer sets to 10 relevant genes in the retinoic acid pathway and 2 endogenous genes for relative quantification. Review the data and select the genes that give the greatest fold change at the time points chosen for absolute quantification.

3) Construct a standard curve from purified amplicons of the greatest fold change samples from the relative quantification. Purchase fluorescein (FAM) labeled TaqMan® probes to perform absolute quantification on the genes of interest. This also serves to confirm data from the relative quantification.

4) Design, write and implement a training exercise to teach graduate students basic relative real-time PCR in a hands-on wet lab environment.

Zebrafish (*Danio rerio*) as A Model Organism For The Retinoic Acid Metabolism Pathway

In the 1970s, Dr. George Streisinger began using zebrafish to study vertebrate development and genetics. Because the zebrafish has a backbone, it is more closely related to

humans than commonly used invertebrate models like *Drosophila melanogaster* or *Caenorhabditis elegans*. They have features that lend themselves well to a laboratory setting because they are easy to maintain, manipulate and observe. Zebrafish are small in size and therefore can be kept together in large numbers. Their eggs are externally fertilized and non-adhesive, making breeding and collection easy. The embryos remain transparent throughout development allowing observation of individual cells. The clutch size from one breeding pair can be up to 200 embryos, which is helpful for mutation studies that typically require many samples. The embryos develop *ex utero* making them more accessible and visible in contrast to the rat or mouse models which have slower *in utero* development. The quick growth and development is also an advantage as they can go from a single cell to a recognizable fish within 24 hours. In contrast mice require a 21 day gestation period. The central nervous system and other organs of the zebrafish are relatively less complex compared to higher vertebrates. The transparency of the zebrafish also makes viewing cell labeling in live organisms possible. Overall the advantages of the zebrafish system, including easy maintenance, external fertilization, high fecundity, transparent embryos, short generation time and rapid development, make it a model organism for developmental studies[28].

Stages Of Zebrafish Development

During zebrafish embryogenesis a stage atlas is used as a reference guide during the time period from fertilization until the embryo hatches. Development begins with the *Zygote period* between 0 and ¾ hpf. The *Cleavage period* lasts from ¾-2 ¼ hpf and covers the first cell division through to the 64 cell stage. It is during this period that the cell number becomes the principal way to stage the embryos. The first round of cell division that runs horizontally occurs at the 64 cell stage (2 hpf).

The *Blastula period* runs from 2¼ -5¼ hpf and begins at the 128 cell stage. In this period staging is based on the relative size of later cells to earlier ones because the orientation of the cleavage planes is less precise. The cell mound also becomes more refractile and becomes grayish in appearance; cell divisions continue to occur roughly every fifteen minutes. The 512 cell stage is the *mid-blastula transition* (MBT) and at 1000 cells the *yolk syncytial layer* (YSL) is formed. This is the first time that the blastomeres are no longer connected to each other or the yolk cell. The YSL will persist throughout embryogenesis. The next stages in the blastula period are the *High* (3 ½ hpf), S*phere* (4 hpf) and *Dome* (4 1/3 hpf). During the dome stage the yolk cell bulges and creates a dome-like shape. *Epiboly* (4 2/3 – 10 hpf) begins in late blastula and continues to the end of *gastrulation* when the yolk is totally covered. The staging during this time is a measure of the percentage at which epiboly is covering the yolk. The stages are 50% epiboly (5 ¼ hpf), shield (6 hpf) and 80% epiboly (8 1/3 hpf). The yolk that is still uncovered during late epiboly is referred to as the yolk plug. The neural plate (9 hpf) and tail bud (10 hpf) lead up to the *Segmentation period* (10-24 hpf). During this time somites are formed, mesodermal segments that occur approximately every 30 minutes and are used for staging for this period. The stages are 1 *somite* (10 1/3 hpf), 5 *somites* (11 2/3 hpf) when the brain appears thicker and optic vesicles begin to grow, 15 *somites* (16 ½ hpf) when the yolk pinches in and adopts a kidney bean shape, and 20 *somites* (19 hpf) when the *lens placode* becomes visible in the developing eye. The majority of cells in a somite become muscle segments. The somites in zebrafish are not transient and the segmental muscle arrangement persists throughout adulthood. Towards the end of this period, body movements occur.

The *Pharyngula period* (24-48 hpf) derives its name from the seven pharyngeal arches, of which the first becomes the jaw and the posterior five become the gills. Staging during this

period is a little more difficult as it is based on the position of the leading tip of the migrating part of the postotic lateral line primordium in the trunk and tail. The distance between the eye and ear of the head-trunk angle are also used to stage the embryos. The *Primula 5* stage (24 hpf) marks a time when the embryo has around 30 somites and the heart starts beating just prior to this stage, erythrocytes can be seen and the blood begins circulating. *Primula 15* (30hpf) and *Primula 25*(36 hpf) are marked by decreasing head-trunk angle (HTA) and decreasing otic vesicle length (OVL). Melanin synthesis begins first in the retinal pigment epithelium and then in the melanophores in the skin.

The *Hatching period* (48-72 hpf) is not synchronous and occurs at irregular intervals during the third day. Development slows down considerably but the development of the gill arches and pectoral fins are characteristic of this period. *The long pectoral fin bud stage* (48 hpf) shows an HTA of 45º and the OVL is ½ . Fin buds flatten out and elongate but have not taken the characteristic fin-like shape yet. The otic vesicle differentiates and melanophores cover the head and trunk. The remaining yolk is about the same size as the developing head and as it shrinks the heart can be seen more easily. Blood is seen circulating throughout the trunk and tail. During the *protruding mouth stage* (72 hpf) the head is nearly in line with the trunk, the HTA is only 25º and the mouth protrudes beyond the eyes. Melanocytes begin developing over the location of the swim bladder and melanophores have accumulated into the four characteristic stripes of the larvae. After this stage is the *Early Larval period* (3-7 dpf) where most of the morphogenesis is complete and the zebrafish is mainly increasing in size. The biggest change on day four is the inflation of the swim bladder. The yolk extention is used up and the larvae start to swim actively. They now show escape responses, respiration and seek and consume food[29] (Figure 1-5).

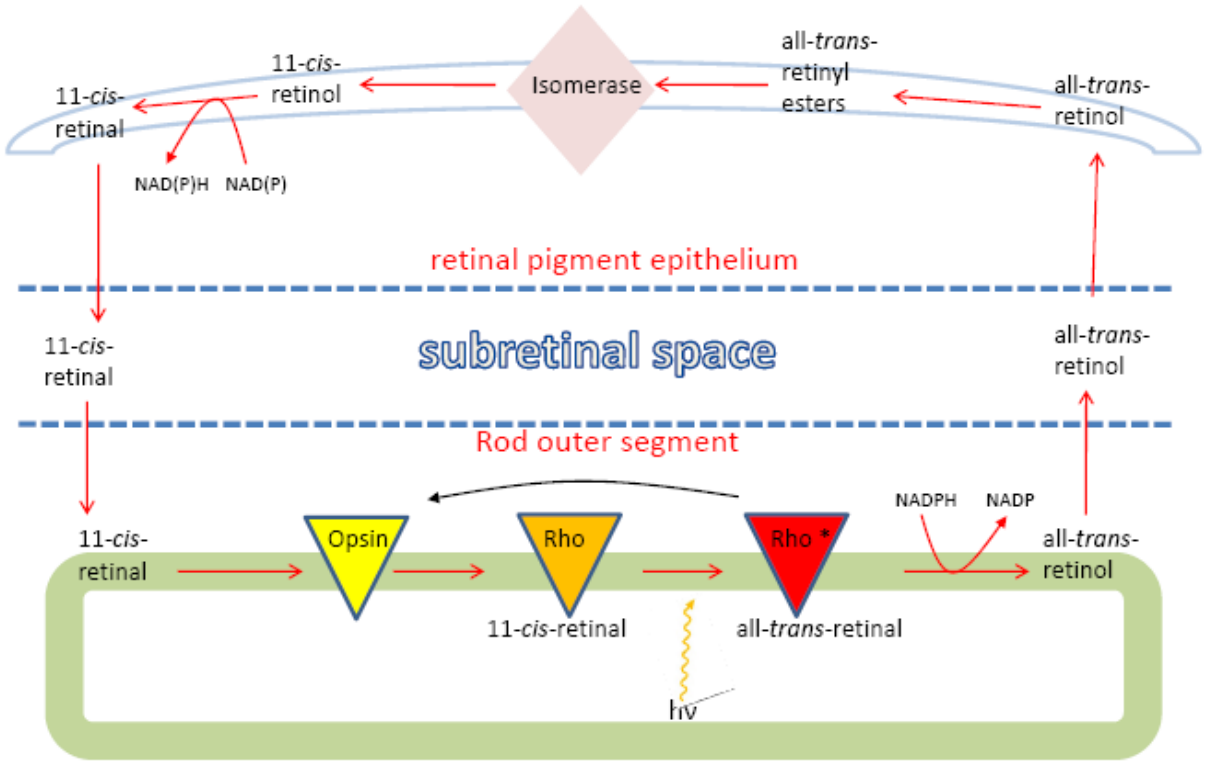

Figure 1-1. The vertebrate rod visual cycle. This depiction illustrates some of the known reactions involved with the regeneration of rod visual pigments. Light (hυ) converts 11-cis retinal bound to rhodopsin to all-trans-retinal and is reduced to all-trans-retinol in the rod outer segment. All-trans-retinol then moves into the retinal pigment epithelium, becomes esterified and converted to 11-cis-retinol by an isomerase and oxidized to 11-cis-retinal. 11-cis-retinal then returns to the rod, regenerates rhodopsin and completes the visual cycle30. [Adapted from Saari, J.C. The sights along route 65. Nat Genet 29, 8-9 (2001).]

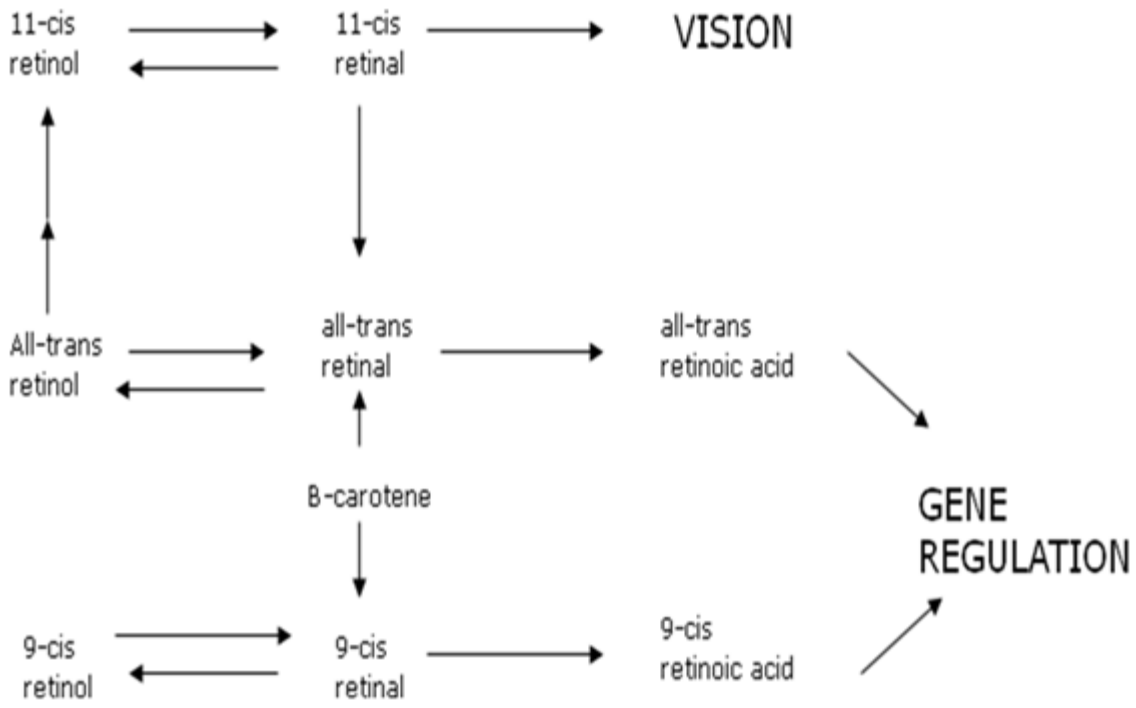

Figure 1-2. Different metabolites of retinoic acid affect gene regulation or vision.

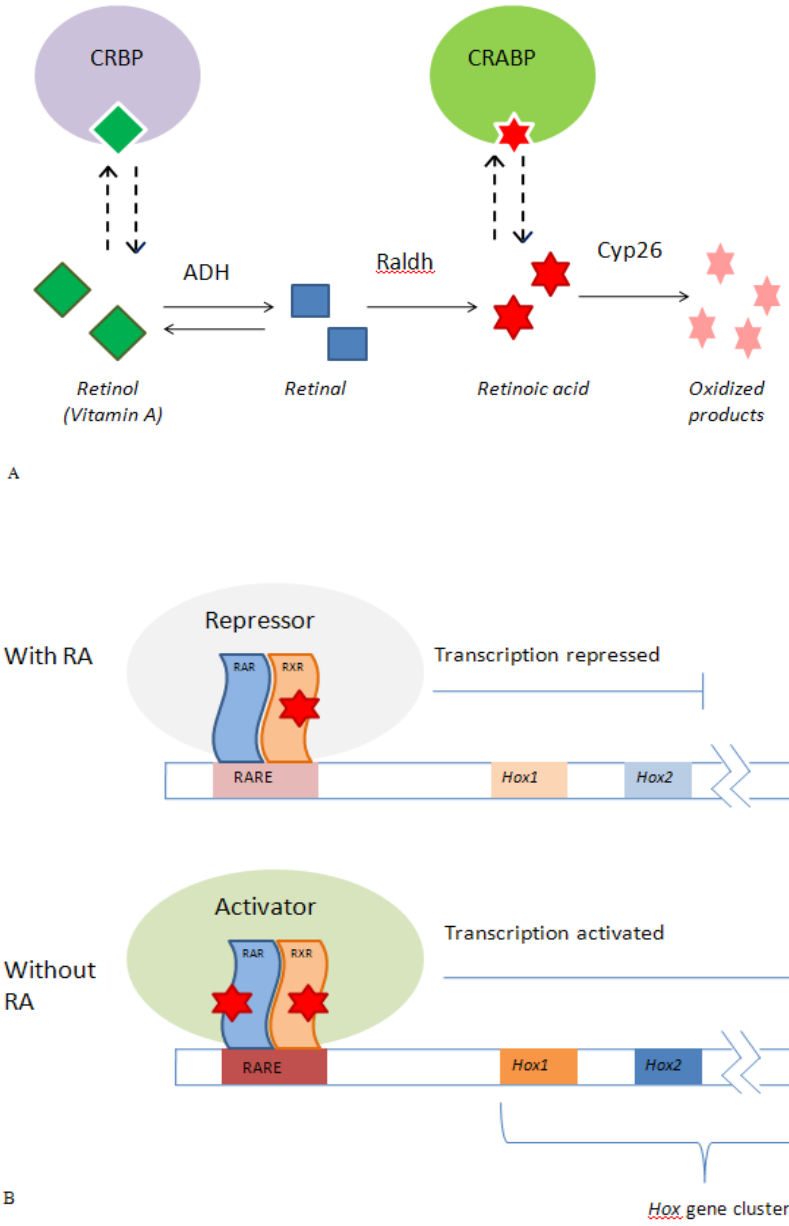

Figure 1-3. Synthesis, degradation and mode of action of retinoic acid. A) Vitamin A is reversibly converted to retinal by aldehyde dehydrogenases. Retinal is irreversibly converted to RA by retinaldehyde dehydrogenases (RALDHs) and eventually degraded by CYP26 enzymes. Cellular retinol binding proteins bind retinol and cellular retinoic acid binding proteins bind the RA. B) RA signaling is mediated when RA binds to retinoic acid receptors (RAR) that then forms heterodimers with retinoid X receptors (RXR). This complex then binds to retinoic acid response elements (RARE) in regulatory regions of target genes. The conformational changes induced when RA is bound leads to histone acetylation and activation of transcription[19]. [Adapted from Marletaz, F., Holland, L.Z., Laudet, V. & Schubert, M. Retinoic acid signaling and the evolution of chordates. *Int J Biol Sci* **2**, 38-47 (2006).]

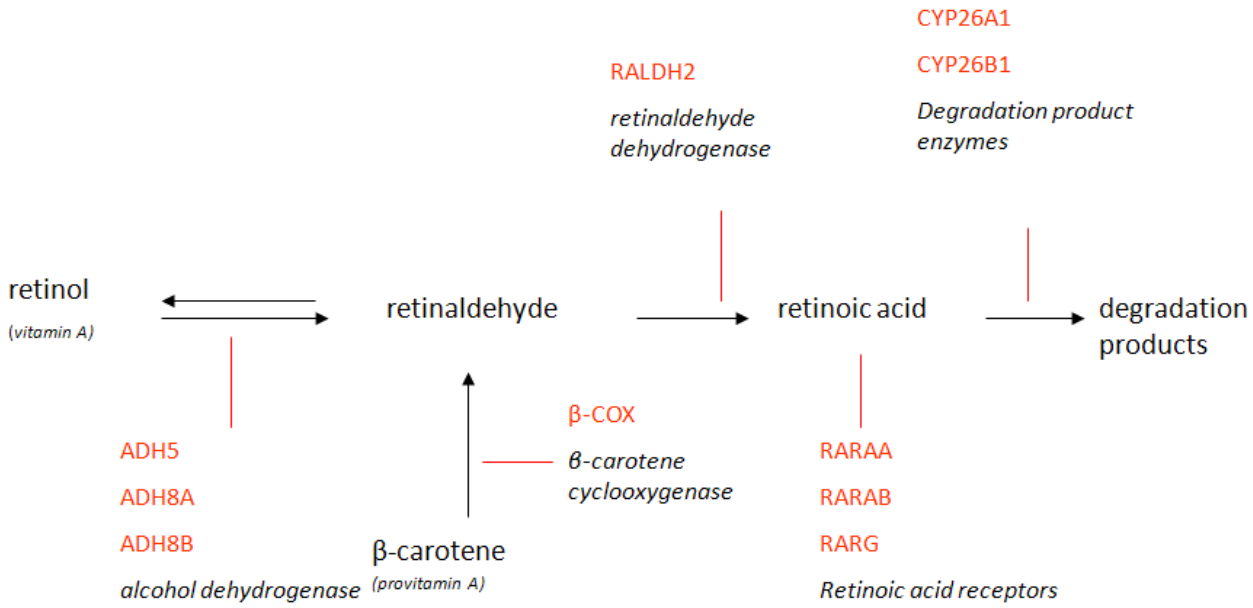

Figure 1-4. Retinoic acid pathway. Target genes of receptors and enzymes that will be investigated using real-time PCR are in red.

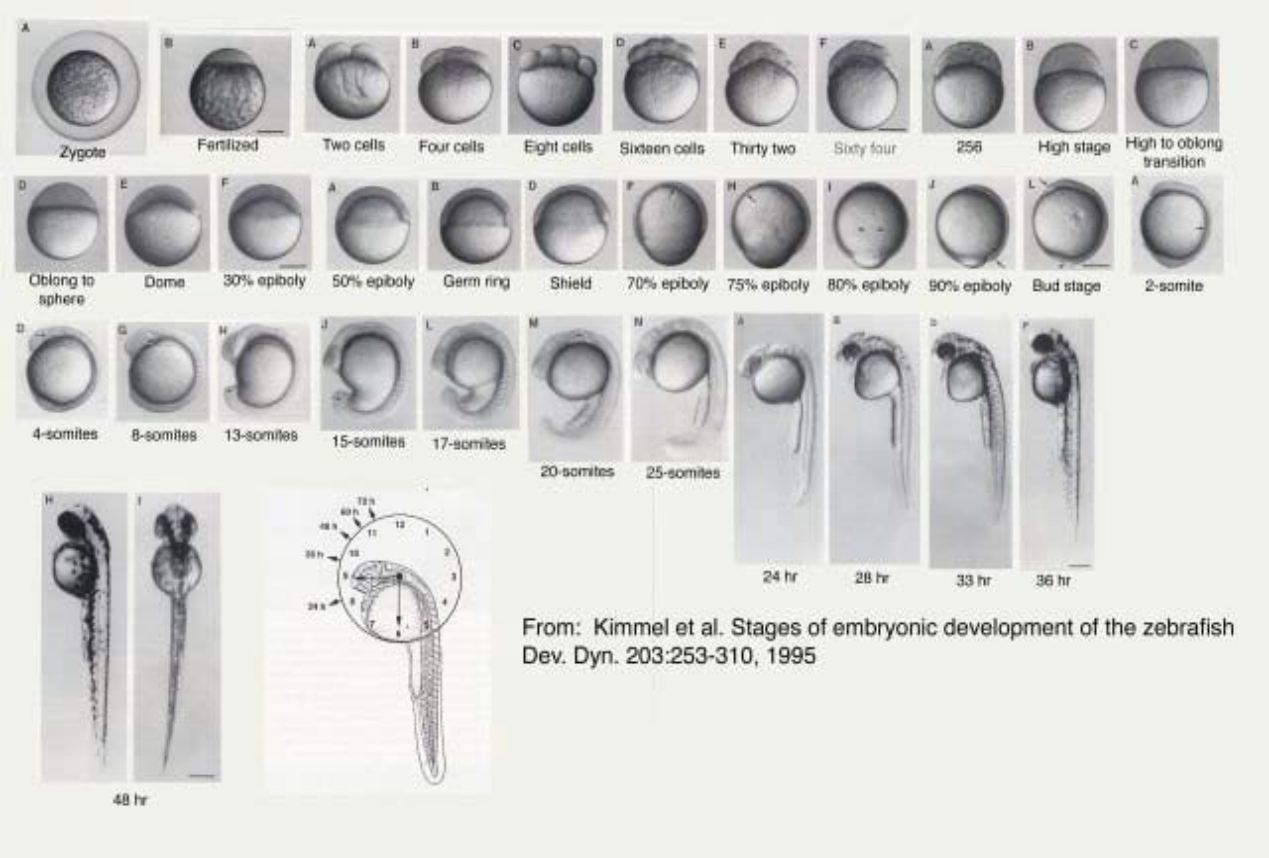

Figure 1-5. Stages and chart of changes in the head-trunk angle (HTA) of early zebrafish development[31] (Reprinted with permission from Kimmel et al.)

CHAPTER 2
MATERIALS AND METHODS

All chemicals were obtained from Sigma-Aldrich (St. Louis, MO) or Fisher Scientific (Pittsburgh, PA), and all primers designed for the SYBR® Green relative quantification were obtained from Eurofins MWG Operon (Huntsville, AL) unless otherwise noted.

Fish Strains And Husbandry

Zebrafish (D*anio rerio*) were maintained at the Whitney Laboratory for Marine Bioscience (St. Augustine, FL). They were raised in 14 hour light and 10 hour dark cycle at a constant temperature of 28º C. The fish were fed 3 times daily with brine shrimp. Males and females in a 1:1 ratio were placed in a breeding tank with a partition between them. Approximately 1 hour after the beginning of the light cycle, the partition was removed. After fertilization the embryos drop through the slats in the bottom of the breeding tank and are collected from the bottom of the holding tank. Embryos are stored in egg water (1.5 mM Instant Ocean sea salt, 0.05% methylene blue fungicide) at 28º C until the desired harvesting time. At harvest embyos are counted, removed from egg water to a cryovial, frozen in liquid nitrogen and stored at -80º C.

RNA Isolation And Quality Determination

RNA Isolation From Embryos And Whole Fish

RNA was isolated from 50 embryos at 5-6 hours post fertilization (hpf), 50 embryos at 24 hpf, 25 embryos at 48 hpf and 25 embryos at 72 hpf using a Qiagen RNAeasy Plus kit with genomic DNA eliminator columns (Qiagen; Valencia, CA). The embryos were lysed and homogenized in 600 µL lysis buffer from the kit using a sample pestle (Research Products International Corp.; Mount Prospect, IL) in a 1.5 mL tube in a liquid nitrogen bath. The total RNA was eluted from the column with 30 µL of NANOpure water (Barnstead; Dubuque, Iowa).

RNA was isolated from a 70 mg slice of whole zebrafish using the Aurum™ Total RNA Fatty and Fibrous Tissue Kit (Bio-Rad; Hercules, CA). Samples were lysed and homogenized in one mL of PureZOL™ RNA isolation reagent (Bio-Rad) with a Tissue Tearor™ variable speed tissue homogenizer (Biospec Products, Inc.; Bartlesville, OK). Elution of total RNA from the Aurum kit column was done twice with 35 µL of NANOpure water each for a total of 70 µL.

RNA was isolated from a second set of samples consisting of 100 embryos at 1.5 HPF, 100 embryos at 5 HPF, 100 embryos at 24 HPF and 60 embryos at 48 HPF using the Aurum kit (Bio-Rad). Samples were lysed and homogenized as described previously. Elution of total RNA from each Aurum kit column was in 35 µL of NANOpure water.

Quality Determination

Determining the quality of the RNA is an essential step prior to any gene expression analysis. To make the most accurate assessment possible, three parameters were considered: Nanodrop readings (NanoDrop Technologies, LLC.; Wilmington, DE) , Bioanalyzer readings (Agilent Technologies, Inc.; Santa Clara, CA) and the RNA Integrity Number (RIN)[32]. RNA concentrations of the samples were determined using a NanoDrop spectrophotometer. Readings are taken at absorbance (A) 230 nm, 260 nm, and 280 nm. Ratios of A260 nm/A280 nm and A260/A230 are displayed with the concentration in ng/µL. All samples had an A260/A280 ratio between 2.0 and 2.1 indicating high purity RNA (Figure 2-1). The integrity of the RNA samples was determined by assessment on an Agilent 2100 Bioanalyzer. All electropherogram summaries and electrophoresis file run summaries of the samples indicate high quality, intact total RNA (Figure 2-2). The RNA Integrity Number (RIN) provided by the Bioanalyzer is an algorithm developed by Agilent Technologies using Eukaryote Total RNA on an Agilent 2100 Bioanalyzer to give information about the integrity of RNA sample[32]. A scale from 1 to 10 is used to determine the RIN, with ten being the most intact and one indicating complete degradation. All

embryo and whole fish total RNA RIN numbers had a minimum reading of 8.2 with the majority of samples in the 9-10 range.

Real-Time PCR

Relative Quantification

Reverse transcription of total RNA (1 µg) to cDNA was done with an iScript ™ cDNA Synthesis Kit (Bio-Rad). In a 0.2 mL PCR tube, 5X iScript reaction mix (4 µL) and iScript reverse transcriptase (1 µL) were mixed with 1 µg RNA for a total reaction volume of 20 µL. The sample was incubated at 25° C for 5 minutes, 42° C for 30 minutes and then 85°C for 5 minutes in a DNA Engine Peltier thermal cycler (Bio-Rad).

Ten sets of primers were designed for genes of interest in the retinoic acid pathway using the Premier Biosoft Beacon Designer 7.0 (Palo Alto, CA). An additional primer set for alpha actin was obtained from literature[33] (Table 2-1). Two of the primer sets, alpha actin (actin) and elongation factor (EF1α) were used as the endogenous controls. The cDNA stock was initially diluted 10 fold in water so that approximately 4 ng of cDNA made from whole fish total RNA were used as the template per well for the primer optimization. Each primer set was tested with a temperature gradient from 7ºC below the melting temperature (TM) to 4ºC above the TM. The final concentration of primers in a 25 µL reaction was 0.2 µM. iQ SYBR® Green Supermix (Bio-Rad) was used at a final concentration of 1X. Each temperature time point was performed in duplicate with whole fish cDNA, with an additional well for the no template control (NTC). Cycling conditions were 95ºC for 3 minutes and then 40 cycles of 95ºC for 10 seconds and gradient determined temperature for 1 minute. A melting curve analysis between 45º C and 90º C confirmed the lack of primer dimers and multiple nonspecific products. Primer sets were chosen based on lowest threshold cycle (C_t), efficiency range of 90% to 105% and a compatible temperature range of 59º C so that all primers sets could be used on a single plate. Each embryo

cDNA was run in duplicate with the same reaction mix conditions as the primer optimization and repeated twice for each of the twelve primer sets to ensure reproducibility between replicates, plates and biological samples. To determine the amount of cDNA that should be used per well with optimized primers, the stock cDNA was then serially diluted 10 fold 8 times. The 2^{nd} through 7^{th} dilutions were run in duplicate with a NTC in a 25 µL reaction mix with 0.2 µM final concentration of primers, 1X iQ SYBR® Green Supermix (Bio-Rad), 4 ng of cDNA and cycling conditions of 95ºC for 3 minutes, 40 cycles of 95ºC for 10 seconds and 59ºC for 1 minute. To replicate similar PCR amplification efficiencies among all the genes with their respective primer set, the 10 fold diluted cDNA was further diluted 10,000 fold for actin, 100 fold for EF1α and 10 fold for all other primer sets. Using the cDNA at these dilutions made the PCR reactions comparable for relative quantification.

Absolute Quantification

To test the ability to make a standard curve from SYBR® Green chemistry amplified product, 20 µL aliquots from RALDH2, RARG, CYP26B1 and EF1α were mixed with 6X loading dye and electrophoresed on a 1.2% agarose and ethidium bromide gel at 80 V for 50 minutes. The bands were excised from the gel and separated from the agarose with a QIAquick Gel Extraction Kit (Qiagen) according to the manufacturer's protocol. A Nanodrop spectrophotometer was used to measure quantity. The sample was then diluted serially 5 fold between 1X 10^7 molecules and 640 molecules. These dilutions were then amplified with iQ SYBR® Green Supermix in triplicate to test standard curve suitability (Figure 2-3). The standard curve to which unknown samples are compared for quantification is defined as the line equation $y = mx + b$ where m is the slope and b is the y-intercept. Theoretically if there is perfect doubling of the template at each cycle then the slope would be -3.32. The threshold line should be placed where the slope is close to this value. Figure 2-3 shows the threshold is properly set as evidenced

by the slope of the line equaling -3.265. A second 20 µL sample of EF1α post amplification product was purified from unused primer and dNTPS using the MinElute PCR Purification kit (Qiagen) according to the kit-provided protocol. The quantity was measured as above and is used as a template for the biotin probe as described in the Northern Blotting section.

The following TaqMan® primer and probe Assay-on-Demand reagents were purchased from Applied Biosystems (Foster City, CA): retinoic acid receptor gamma a (assay ID Dr03176411_s1), aldehyde dehydrogenase 1family member A2 (assay ID Dr03131675_g1) and cytochrome P450, family 26, subfamily b, polypeptide 1 (assay ID Dr03088544). The Applied Biosystems High Capacity cDNA Reverse Transcription Kit (Applied Biosystems) was used to make complementary cDNA that was subsequently diluted 10 fold in water. Duplicate reactions were set up so that each well contained 1 µL of diluted cDNA, 1 µL of the TaqMan® primer and probe mix, and 1X concentration of TaqMan® Gene Expression Master mix (Applied Biosystems). Cycling conditions were 50ºC for 2 minutes, 95ºC for 10 minutes then 40 cycles of 95ºC for 15 seconds and 59ºC for 1 minute. An aliquot of 20 µL from 2 identical wells with the lowest C_t values for RALDH2, RARG and CYP26B1 were electrophoresed on a 1.2% agarose and ethidium bromide gel. The two bands for each gene were excised from the gel (Figure 2-4) and separated from the agarose with a QIAquick Gel Extraction Kit (Qiagen) according to the kit-provided protocol and combined. A Nanodrop spectrophotometer was used to measure quantity. The sample was then diluted serially five- fold between $1X10^7$ molecules and 640 molecules and the dilutions were used to create a standard curve. Triplicate reactions were set up in 20µL volumes for each biological replicate of adult fish, embryo cDNA and standard curve dilutions, with the same primer concentrations and cycling conditions as previously described. Unknown samples are compared to the values of the standard curve for quantification.

In summary, the SYBR® Green chemistry was used initially with RALDH2, RARG and CYP26B1 primers on adult fish to test feasibility of using gel purified cDNA to construct the standard curve as shown in Figure 2-3. For absolute quantification by real-time PCR, SYBR® Green chemistry, EF1α primers and adult fish cDNA were used to produce a standard curve. TaqMan® chemistry, RALDH2, RARG and CYP26B1 primers and 24 hpf embryo RNA were used to construct standard curves for their absolute quantification. The decision to use two different chemistries was a result of the unavailability of pre-made EF1α TaqMan® primers and probes from Applied Biosystems (Figure 2-5).

Northern Blotting

Electrophoresis And Transfer to Membrane

The NorthernMax® (Ambion) formaldehyde-based system for Northern blots kit was used. Agarose (1 gram) was melted in 90 mL of water and 10 mL of Denaturing Gel buffer were added. The gel was poured to a thickness of approximetly 0.6 mm. Each gel contained one lane of marker and one lane of whole fish total RNA. A marker was prepared by combining 2 µL of the BrightStar® Biotinylated RNA Millennium™ Markers (Ambion) with 8µL of nuclease free water and 10 µL of 2X RNA Sample Loading Buffer (Fisher Bioreagents). The whole fish RNA (10 µg) was also prepared to contain a final concentration of 1X RNA Sample Loading Buffer in a 20 µL volume. Both whole fish RNA sample and the RNA marker sample were heated to 80º C for 10 minutes and then chilled on ice for 2 minutes. The entire 20 µL of both samples were loaded onto the gel and electrophoresed at 80V for approximately 1 hour (Figure 2-6). The gel was transferred to BrightStar Plus positively charged membrane (Ambion) via downward capillary action and NorthernMax kit transfer buffer according to the kit-provided protocol and left to transfer for 16 hours. After transfer, the RNA was crosslinked to the damp membrane using ultraviolet light in a GS Gene Linker™ UV Chamber (Bio-Rad).

Probe Labeling

The NEBlot® Phototope® Kit (New England BioLabs, Inc.; Ipswich, MA) was used to incorporate biotin into the hybridization probes by a random primer reaction using the Feinberg and Vogelstein method[41]. Biotinylated random octamers primed DNA synthesis *in vitro* from single stranded DNA. Klenow enzyme then synthesized the rest of the DNA for the probe. To a final volume of 34 µL, 50 ng of purified standard curve PCR samples from the Absolute Quantification Section were suspended in nuclease-free water. From the NEBlot Photope kit, 2 µL of control DNA were added to 32 µL of nuclease-free water. The samples were heat denatured in boiling water for 5 minutes. From the NEBlot Phototope kit 2 µL of control DNA were added to 32 µL nuclease free water. Both were then chilled on ice for 5 minutes and the following reagents were added to each tube: 10 µL of 5X labeling mix containing biotinylated random octamers, 5 µL of a dNTP mix containing dNTPS and biotin-dATP and 1 µL of Klenow fragment. The reactions were incubated at 37º C for 90 minutes and then terminated by the addition of 5 µL of 0.2 M EDTA, pH 8.0. The reaction products were purified with the MinElute PCR Purification Kit (Qiagen) according to the kit-provided protocol and eluted in a final volume of 20 µL of 1X TE.

A dot blot was made to determine the level of probe biotinylation. Serial ten-fold dilutions were made of the sample probe, control probe and the biotinylated 2-log DNA ladder in 0.1 N NaOH and 1 µL of each dilution was spotted onto BrightStar Plus (Ambion) positively charged membrane. After the dots dried the membrane was crosslinked with 250 mJoule UV light. Membranes were processed according to the protocol in the detection section.

Hybridization

The Northern blot membrane was placed into a 50 mL polypropylene conical tube (NUNC; Rochester, NY) that was lined with Flow Mesh (Diversified Biotech; Boston, MA). To the

conical tube, 10 mL of ULTRAhyb prehybridization and hybridization solution (Ambion) were added and incubated for 1 hour at 42ºC in a Bambino Hybridization Oven (Boekel Scientific; Feasterville, PA). Based on the 50 ng of starting material and the 90 minutes of labeling incubation, it is estimated that the biotinylated probe concentration should be approximately 20 ng/µL. The probes, 10 µL each, were heat-denatured in 50 µL of 10 mM EDTA at 90º C, then 500 µL of the prewarmed 42º C ULTRAhyb solution (Ambion) were added to the tube. The entire contents of the probe reactions were transferred to the tube containing the membrane. The probe was hybridized to the membrane at 42º C for 16 hours.

Low stringency washes (2X SSC, 0.1% SDS) were done twice at room temperature for 5 minutes each. High stringency washes (0.1X SSC, 0.1% SDS) were done twice at 42º C for 15 minutes each. The blot was removed from the conical tube and sealed in a hybridization bag with pour spout (Roche; Indianapolis, IN).

Detection

The Phototope®-Star Detection kit (New England BioLabs) was used to process the blot. All steps were carried out for 5 minutes with moderate shaking at room temperature in a hybridization bag. The detection protocol consisted of blocking (5% SDS, 25 mM sodium phosphate, pH 7.2, 125 mM NaCl), streptavidin incubation, wash 1 twice (0.5% SDS, 2.5 mM sodium phosphate, pH 7.2, 12.5 mM NaCl), biotinylated alkaline phosphatase incubation, blocking, wash 2 twice (100 mM Tris-HCl, 100 mM NaCl, 10 mM $MgCl_2$, pH 9.5) and 1X CDP-Star Assay Buffer. The blot was then sealed into the hybridization bag and exposed to film for different lengths of time until the desired exposure was reached. An average of between 15 seconds and 1 minute produced a well defined marker lane and low background. The film was developed in a Konica SRX-101A tabletop cold water film processor.

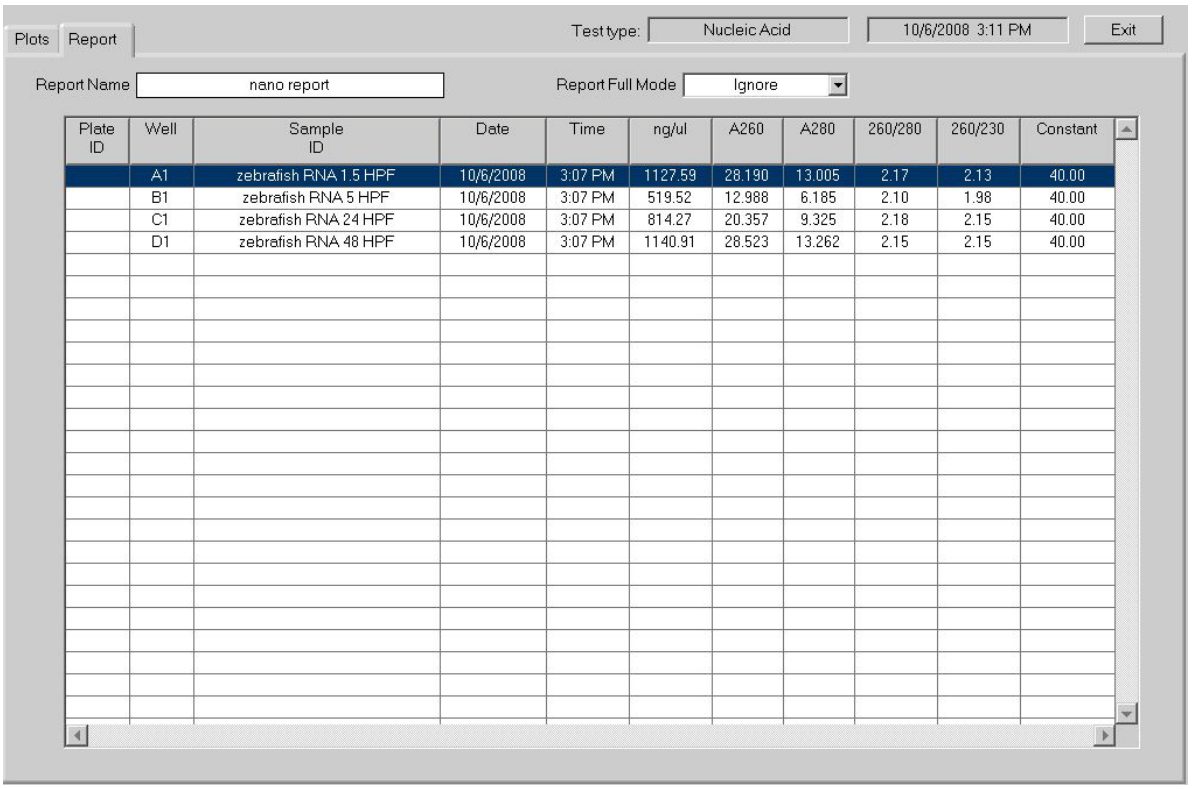

Plate ID	Well	Sample ID	Date	Time	ng/ul	A260	A280	260/280	260/230	Constant
	A1	zebrafish RNA 1.5 HPF	10/6/2008	3:07 PM	1127.59	28.190	13.005	2.17	2.13	40.00
	B1	zebrafish RNA 5 HPF	10/6/2008	3:07 PM	519.52	12.988	6.185	2.10	1.98	40.00
	C1	zebrafish RNA 24 HPF	10/6/2008	3:07 PM	814.27	20.357	9.325	2.18	2.15	40.00
	D1	zebrafish RNA 48 HPF	10/6/2008	3:07 PM	1140.91	28.523	13.262	2.15	2.15	40.00

Figure 2-1. Nanodrop spectrophotometer data of RNA samples from 1.5, 5, 24 and 48 hpf embryos.

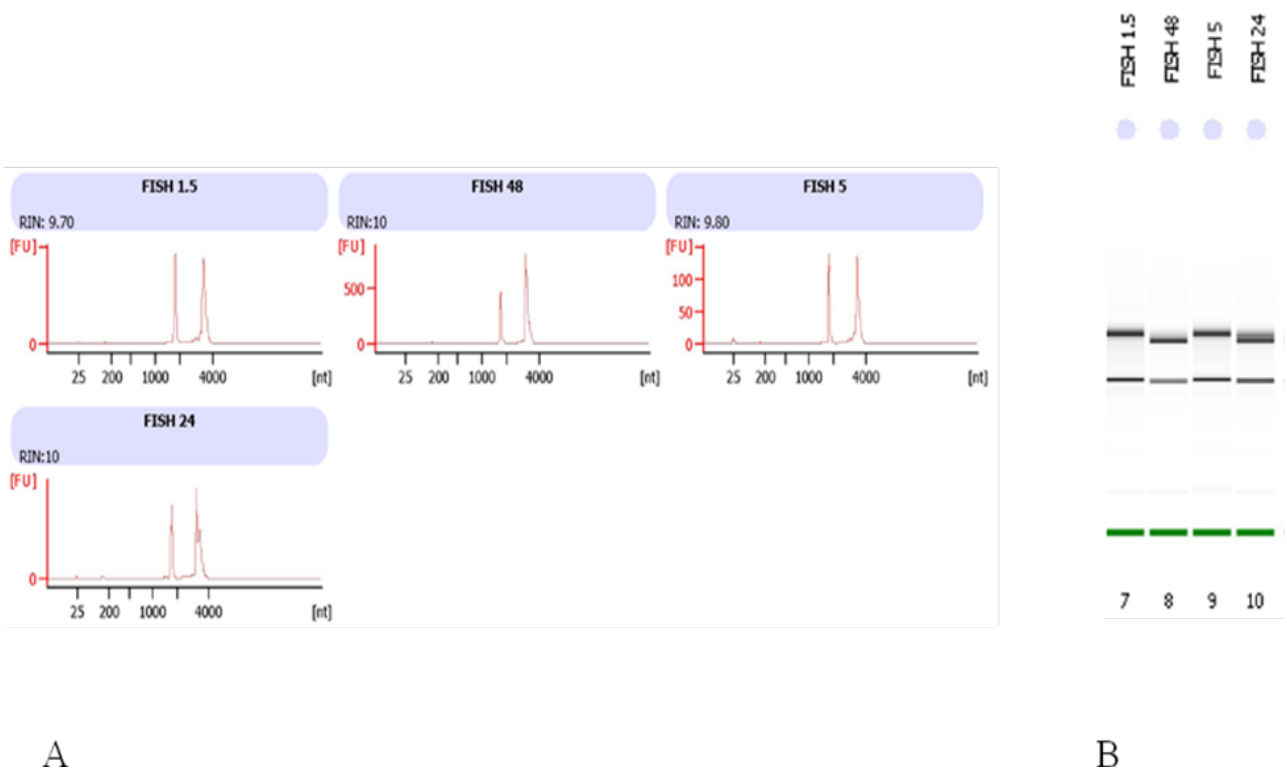

Figure 2-2. Quality determination of total RNA. A) Bioanalyzer Electropherogram results with accompanying RNA Integrity Number. B) Bioanalyzer electrophoresis file run summary.

Table 2-1 Retinoic acid genes and SYBR® Green primer sequences

Gene name	Accession Number	Abbreviation	Primer Sequence (5'-3')
Beta-carotene monooxygenase	NM_131798	BCOX	(F) TCAGCCACACCATCCCAGAC
			(R) ATGAGAAGCCACGATACTTACAGG
Alcohol dehydrogenase 5	NM_131849	ADH5	(F) CTGGTGAACGACTACATGAACAAG
			(R) AGGACGAGGCTCAGGCTTC
Alcohol dehhydrogenase 8a	NM_001001946	ADH8A	(F) CAAGGGTGAGTGGCAAGAC
			(R) AAGAACAGGTGGATGATGGTG
Alcohol dehydrogenase 8b	NM_203460	ADH8B	(F) AAGTGCTGATAGAAATGACCAATG
			(R) AGTCCGTATTAGTGTATCCAACC
Aldehyde dehydrogenase a2	NM_131850	RALDH2	(F) GAGACAGTGCTTACCTTG
			(R) CCATCCAGCGTAATATCG
Retinoic acid receptor a	L03398	RARAA	(F) ATCCATCGCTCTGTTAAATCTC
			(R) GTTCACATCCACACTCTCATAC
Retinoic acid receptor b	L03399	RARAB	(F) CTTCTGCTGAACTGACTTAC
			(R) TTCTCCGAAAGTAAATGTAGC
Retinoic acid receptor g	S74156	RARG	(F) GGTGTTGTTATTGTTGTTTTG
			(R) CAGAGCCTCCATACAGTC
Cytochrome P450 26a1	NM_131146	CYP26A1	(F) TGTTCTCCTTGCCAATCG
			(R) AGCGTCTTTGTATTTCTGC
Cytochrome P450 26b1	NM_212666	CYP26B1	(F) TTGTTCAGCACCTTCCAG
			(R) AGCACATCAAGAGCATCAG
Elongation factor 1 alpha	NM_131263	EF1α	(F) TCAAGAAGATCGGCTACAAC
			(R) GGGCATCAAGAAGAGTAG

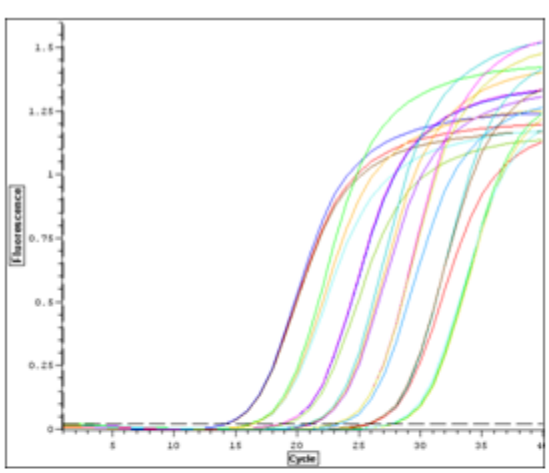

A

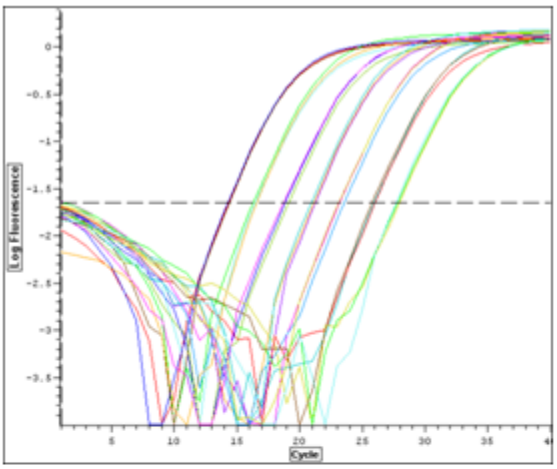

B

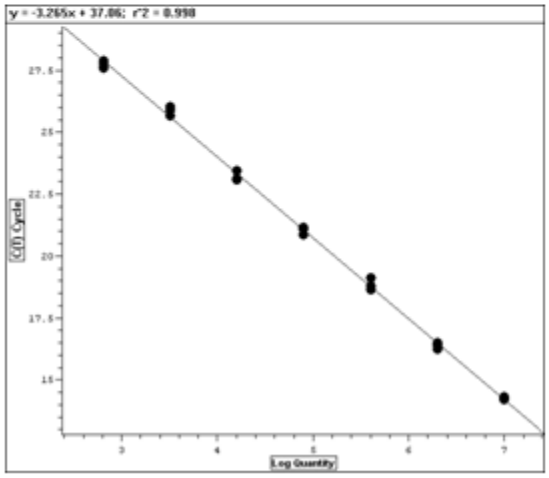

C

A1	105.61%	14.26	1e+007
A2	113.14%	14.31	1e+007
A3	105.05%	14.20	1e+007
B1	101.78%	16.24	2e+006
B2	102.54%	16.41	2e+006
B3	118.40%	16.50	2e+006
C1	101.26%	18.81	4e+005
C2	100.90%	19.12	4e+005
C3	88.16%	18.66	4e+005
D1	106.02%	21.08	8e+004
D2	108.57%	21.16	8e+004
D3	108.15%	20.88	8e+004
E1	99.59%	23.14	1.6e+004
E2	104.80%	23.45	1.6e+004
E3	95.12%	23.09	1.6e+004
F1	106.77%	25.88	3200
F2	106.15%	26.02	3200
F3	99.04%	25.68	3200
G1	104.63%	27.90	640
G2	96.49%	27.74	640
G3	102.16%	27.60	640

D

Figure 2-3. SYBR® Green standard curve. This figure is an example of standard curve created with SYBR® Green primers for RALDH2 and gel purified amplification products as the serially diluted template. A) This fluorescence versus cycle number view shows the dotted threshold line in the default position very low on the curve. B) This is the log view of the same data in A which shows the default threshold line placed in the linear portion of the curve. C) This standard curve graph plots the base-10 logarithm of copy number vs. the C_t value. The line equation above shows a slope of -3.265 which indicates close to perfect template doubling during each amplification cycle and a properly placed threshold line. D) Efficiency percentage, C_t value and copy number at each well used to create the standard curve.

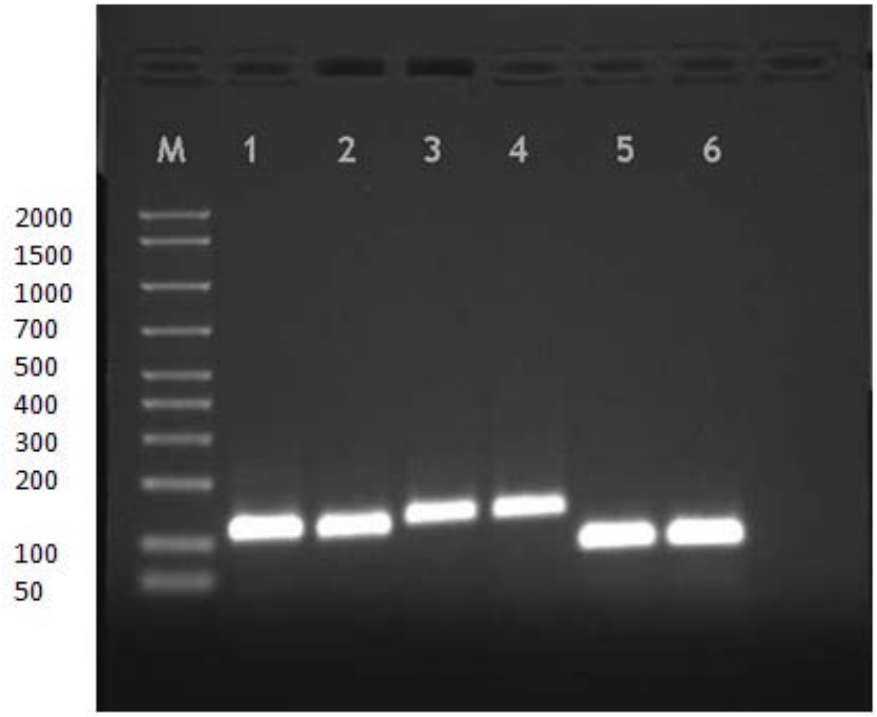

Figure 2-4. Gel image of amplified product used for TaqMan® standard curve. Agarose (1.2%) and ethidium bromide gel image of 20 µL per lane of amplification product resulting from real-time PCR with TaqMan® primers and probes (Applied Biosystem). Lane M-Amplisize molecular ruler 50-2,000 bp (Bio Rad), lanes 1 and 2 are RALDH2 (122 bp), lanes 3 and 4 are RARG (133 bp), lanes 5 and 6 are CYP26B1 (83 bp).

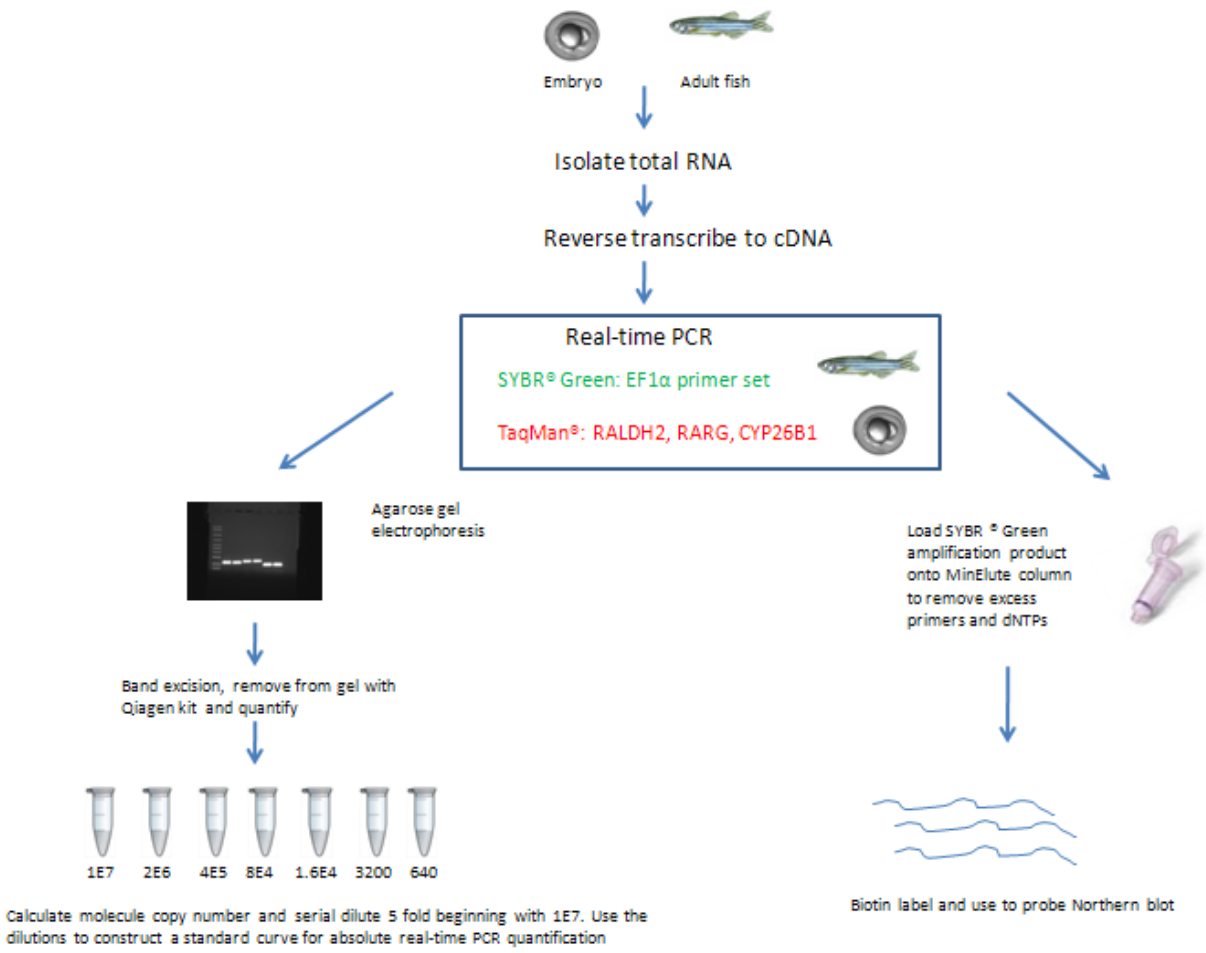

Figure 2-5. Work flow for standard curve construction and Northern blot probe template preparation.

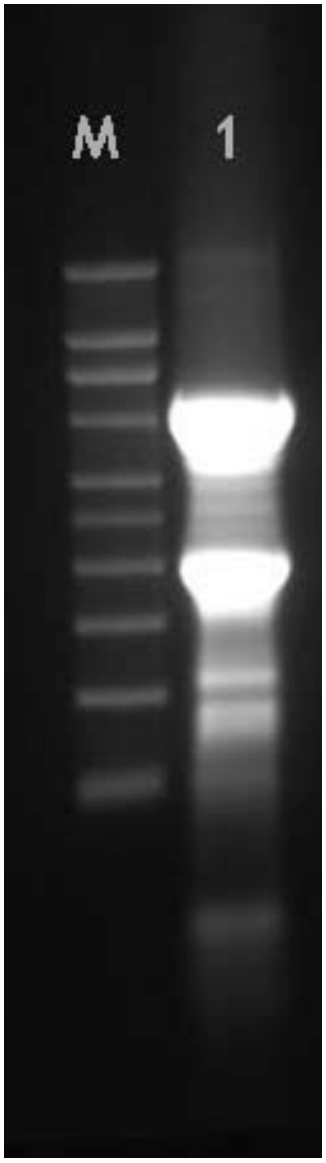

Figure 2-6. Gel image of RNA for Northern blot. This is an image of denaturing RNA gel prior to downward capillary transfer to membrane. Lane M is BrightStar Biotinylated RNA Millennium Markers 0.5 to 9 kb (Ambion), lane 1 is 10 µg of total RNA from adult zebrafish.

CHAPTER 3
RESULTS

Real-Time PCR And *In Situ* Hybridization

Until recently, in situ hybridization (ISH) has been most commonly used to determine presence and location of a particular mRNA in a tissue or organism. This powerful technique permits the study of macroscopic distribution and cellular localization of DNA and RNA sequences in a heterogeneous cell population[34]. Gene expression changes during development are readily observed and the method yields fewer false positive and negative results than immunohistochemical techniques. Proper controls are essential to rule out non-specific binding. Real-time PCR offers an attractive alternative because of its ability to detect and quantify the target with greater specificity and speed at a lower cost, with less time required to master technical skills, making it particularly well suited for a student laboratory exercise. One study comparing chromogenic tyramide-signal-amplified ISH (CISH), conventional PCR and real-time PCR of human papilloma virus (HPV) from archival paraffin-embedded tumors showed that real-time PCR was able to detect the HPV accurately a greater percentage of times than both ISH and conventional PCR and also to quantify the viral load[35]. Applications for disease state detection or screening in a high throughput environment have become routine.

The detection of RA by in situ hybridization on zebrafish embryos has precedence. RALDH2 in the wild type 5 somite stage embryo (12-14 hpf) is shown to be expressed in the anterior paraxial mesoderm[36]. RARG during the 1-4 somite stage (10-12 hpf) is found to be expressed in the epidermis, neural crest, anterior spinal cord, posterior neural plate and the tail bud[37]. CYP26B1 during the same 1-4 somite stage in wild type zebrafish appear in the presumptive rhombomere 3[38]. This information is valuable to demonstrate where in the tissue

these mRNA sequences are located but does not determine the exact amount or give data for earlier stages in the embryo's development.

SYBR® Green Real-Time PCR Analysis

Two different types of real-time PCR chemistries were used in this thesis. SYBR® Green was first chosen to develop the screening panel of twelve different primer sets. The SYBR® Green dye works by binding to all double stranded DNA which then emits a higher level of fluorescence. The greater the amount of product the more light is emitted. SYBR® Green is a good choice for general screening of transcripts prior to moving to probe based assays. It does however require primer optimization for temperature, amount of starting material and similarity in efficiency to be used in relative quantification. Relative quantification is used when comparing the amount of target molecules in comparable samples. The samples must be normalized and have similar PCR efficiencies of sample amplification. The efficiency of a reaction is based on the percent of template that was amplified in each cycle and is primarily an indication of how well the PCR reaction has proceeded. An efficiency close to 100% is the best indicator of a robust and reproducible assay and between 90 and 105% is considered a good range. When considering data for one sample set relative to another, the samples must first be normalized to an endogenous control prior to comparing the fold change difference between them. The endogenous control is usually a housekeeping type message that is present in high copy number. Frequently the template for the endogenous control primers will require a greater dilution in order to achieve similar efficiencies with the other amplified messages. In this study, all the primer sets annealed with similar efficiency at the same temperature and as determined by melting curve analysis did not form dimers or non-specific products. There are several mathematical methods to calculate the relative differences between samples. These include the Livak method, the delta C_t method with reference gene and the Phaffl method. Each method has

advantages and disadvantages and is based on certain assumptions to be made in order for the analysis to be valid[39]. The preliminary screening of the twelve primer sets was on samples that included adult fish and 5 hpf, 24 hpf and 48 hpf embryos. The non-normalized data were compared to the EF1α of the adult fish sample (Figure 3-1). The object of this first screening was to see if there were significant enough fold changes in any of the messages at these time points to warrant further investigation. Each sample and primer set is run in duplicate and the relative difference between adult fish EF1α and all other samples is expressed as a fold change on the y axis. The bands extend downward from the x axis because all the other amplified products are present in lower amounts than the EF1α. Significant fold changes seem to be apparent for ADH8A, RARG and CYP26A1 at 5 hpf and Cyp26A1 at 24 hpf. Even though non-normalized data is limited in providing relative expression information, these encouraging results showed enough fold change variation to warrant further evaluation of the data sets to include the normalization to endogenous controls.

Data Analysis With Relative Expression Software Tool

The Relative Expression Software Tool (REST) was developed in 2002 by Pfaffl *et al.* to compare expression of several genes at the C_t level. C_t is terminology from Applied Biosystems to indicate the threshold cycle of the real-time PCR reaction. It is defined as the cycle when sample fluorescence exceeds a chosen threshold above background fluorescence. The relative expression ratios between samples and control groups with multiple data points are compared. Mathematically, target genes normalized to a reference gene by C_t values are compared with each other. A standalone version that does not run on Excel or Visual Basic can compare unlimited target and reference genes using a newly developed bootstrapping statistical tool and graphical output showing 95% confidence intervals. This standalone version was used for the analysis in this thesis and features a visual representation of gene variation in the form of a

whisker box-plot capable of highlighting issues like distribution skew and a results table to summarize the test information, including reaction efficiency, expression, standard error, 95% confidence interval and hypothesis testing [P(H1)] (39). Since in this study only a single set of data was analyzed for 5 and 24 hpf embryos, the full benefits of REST analysis are not demonstrated in Fig 3-2. A more complete analysis is beyond the scope of this thesis.

Nevertheless, the data in Fig 3-2 indicate that of the twelve genes analyzed the most significant changes occurred in expression of RALDH2, RARG and CYP26B1. The raw C_t values for 24 hpf and 5 hpf of one of the sample sets was entered into the REST program (Figure 3-2). Based on the whisker-box plot, the normalized values for RALDH2, RARG and CYP26B1 diverged more from the normalized EF1α and Actin endogenous controls than the other normalized samples. This indicates that the expression of these genes is at a greater fold change or ratio from the other normalized genes.

Reproducibility Of Results

To confirm and validate that the fold changes observed were reproducible, real-time PCR was completed twice on biological replicates at overlapping time points with each sample in duplicate. The duplicate C_t values were averaged and graphed in Excel (Figure 3-3). A visual comparison of the different amplifications between the EF1α, actin and the other 10 genes of interest indicate the greatest C_t value differences occur between 5 hpf and 24 hpf for RALDH2, RARG and CYP26B1 using SYBR® Green chemistry. These data seem to agree with the results from the REST analysis. Acquiring the same results within and between the biological replicates as well as between the REST data and Excel graph provided confidence that there is a measurable, reproducible fluctuation of gene expression in early zebrafish development for these genes.

Absolute Quantification With TaqMan® Primers And Probes

Based on the Excel graph of real-time C_t values and REST data, reproducible and significant fold changes for RALDH2, RARG and CYP26B1 are detected. To determine the magnitude in a specific and quantitative way, TaqMan® primers and probes were purchased from Applied Biosystems for the three genes of interest (GOI). Two to three replicates were done for each of the mRNAs of interest, RALDH2, RARG and CYP26B1, at 1.5, 5, 24, 48, and 72 hours post fertilization. Quantitative real-time PCR was performed as detailed in the Materials and Methods section. Briefly, 1 µg of total RNA from embryos at the different time points was reverse transcribed to cDNA and amplified with FAM-labeled TaqMan® primer and probes. A standard curve of known copy number for each of the GOI was constructed from gel purified amplified products. Any cDNA sample expressing the target gene can be used for the standard curve after it has been assessed for concentration, converted to a copy number value based on molecular weight, and diluted to a range in which the unknown will be compared. A standard curve and absolute quantification were also completed for the EF1α endogenous control using SYBR® Green chemistry. The result of this analysis gave an absolute copy number of each GOI and for each biological replicate and primer/probe combination. Of interest here, the most significant changes in levels were seen between 5 and 24 hpf. The averaged results with standard deviations for 5 hpf and 24 hpf were used to construct a bar graph (Figure 3-4). Collectively these data suggest that there are approximately 100, 2 and 3 fold increases for RALDH2, RARG and CYP26B1 respectively. These results indicate that this method can be used to detect relative changes in gene expression for key proteins associated with the retinoic acid metabolic pathway during early development of zebrafish.

Northern Blot

In an attempt to validate the real-time PCR results, Northern blot analysis was performed. The question here is whether or not this method can be used to confirm the relative fold change seen by real-time PCR for the GOI during early zebrafish development. Northern blotting is a well known standard method of detection and relative quantification of mRNA levels. It is the preferred method to determine transcript size and alternatively spliced RNAs. The average number of embryos per time point was between 25 and 50, yielding approximately 6-8 µg of total RNA. Although this quantity is adequate for real-time PCR, it was necessary to ask whether or not this amount was sufficient for meaningful Northern analyses. As a control for the embryo studies, adult fish total RNA was first used for a Northern blot. Also by probing total adult fish RNA immobilized on a membrane with biotin labeled probes made from a SYBR® Green amplified cDNA template (Figure 3-5), the transcript size can be confirmed.

To determine the activity of the probe based on the incorporation of biotin, a dot blot was completed as described in the materials and methods section. The amount of labeled probe and the amount of biotin incorporated must be in a sufficient amount to ensure successful hybridization and detection. Two controls provided with the biotin labeling kit are included on the blot as a reference. Biotinylated 2-Log DNA Ladder should be visible down to the 10^{-3} (1 ng/µL) dilution and the biotinylated lambda control should be visible within the 10^{-5}– 10^{-6} range (500-50 fg/µL). A probe was considered to have adequate incorporation of biotin if dots were visible between (1 ng/µL) of the 2-Log DNA Ladder and (50 fg/ µL) of the lambda control. A determination of the approximate concentration of biotinylated DNA is based on the amount of starting template and length of reaction time. All probe concentrations were estimated to be 20 ng/µl (Figure 3-6). In addition to the limitations of probe activity, other factors can negatively impact a Northern blot including the transfer efficiency of the RNA from the gel and the

saturation limitations of the membrane. The laboratory gel apparatus used permitted a total RNA sample of 10 µg in a 20 µL volume to be loaded per lane. Using the number of molecules per µL as determined by TaqMan® absolute quantification, and molecular length, the amount of target message available on the gel for the probes for each GOI and the endogenous control were calculated (Figure 3-7). The labeling of probe was efficient and adequate as determined by the dot blot; they all were visible in the desired concentration range, and biotin incorporation was similar among them. For hybridization, 200 ng of labeled probe was used per 10µg of total RNA which is at least a thousand fold molar excess over the mRNA targets. Using the non-radioactive biotin streptavidin labeling and detection procedure, an amount of message in the total RNA present at a level of approximately 1 pg would be at the lower limit of detection with the CDP-star substrate[40]. It was determined that only the EF1α endogenous control has enough message present in 10 µg of adult fish total RNA to be detected because most likely the entire Northern blot procedure was not 100% efficient . To confirm the calculation, a blot was processed for each sample according to the Materials and Methods section in chapter two. The Northern blot results confirmed the calculations and only the EF1α was detected at the transcript length indicated by NCBI database for that accession number (Figure 3-7). The Northern blot analyses in Figure 3-8 demonstrate that of the adult fish mRNA only EF1α can be detected. Since the amounts of all four mRNAs in adult fish (Figure 3-7) are up to ten-fold greater than those from embryos at 5 and 24 hpf (Figure 3-4), Northern analyses clearly could not be used to validate the real-time PCR data.

Aliquots of the templates used for the Northern blot probe construction were sent to the ICBR DNA Sequencing Core facility along with the forward primer for each. Sequencing was performed for all samples in only one direction since they were under 200 base pairs in length.

An alignment of the predicted and actual sequence shows that the probe sequence is confirmed (Figure 3-9), and demonstrates the accuracy and specificity of amplification during the real-time PCR assay.

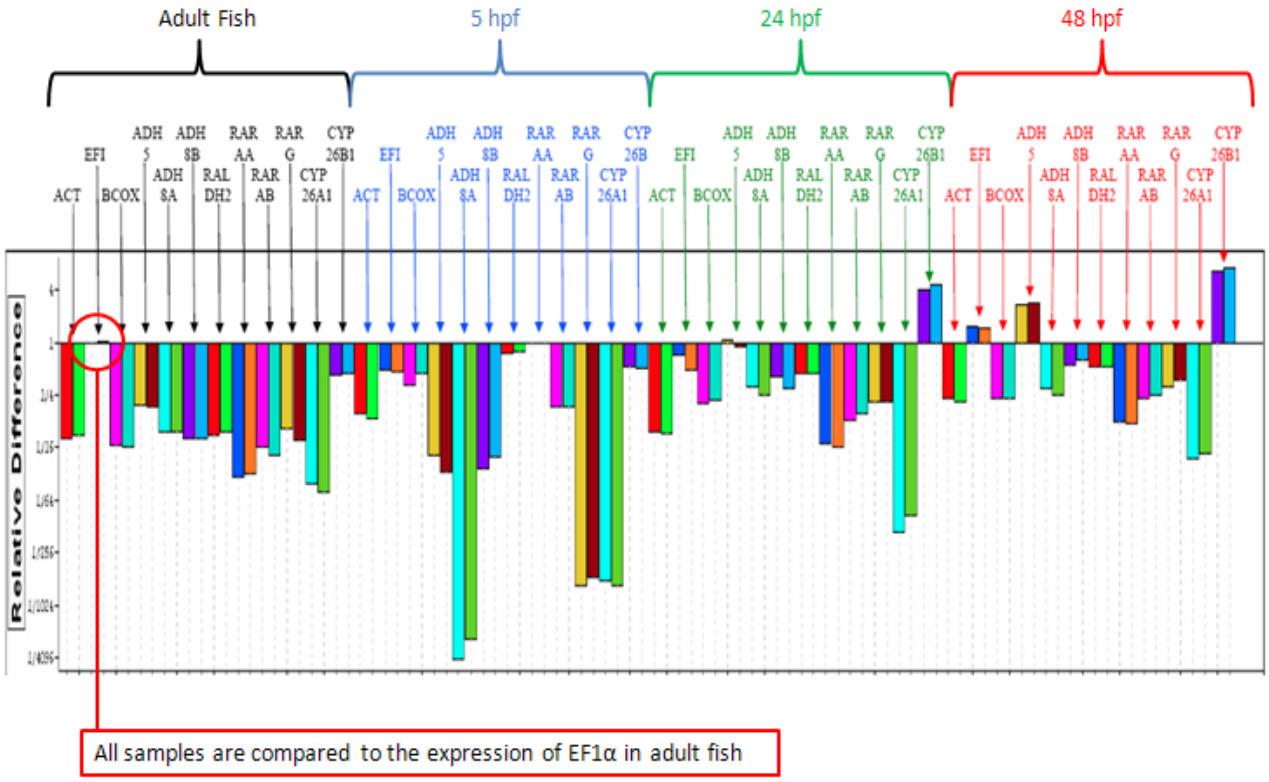

Figure 3-1. SYBR® Green real-time PCR on adult fish and 5 hpf, 24 hpf and 48 hpf embryos with all 12 primer sets. Graphical output shows the C_t values compared between the EF1α of adult fish and embryos at the 3 time points with the 12 different primer sets. Some of the largest fold changes are seen between EF1α and ADH8a 5 hpf, RARG 5 hpf and CYP26A1 5 + 24 hpf. The bars extend downward because the EF1α is in greater abundance.

Results

Gene	Type	Reaction Efficiency	Expression	Std. Error	95% C.I.	P(H1)
actin	REF	0.96	0.696	0.670 - 0.723	0.652 - 0.743	0.927
EF1	REF	0.9	1.437	1.423 - 1.451	1.420 - 1.455	0.714
BCOX	TRG	0.95	0.100	0.088 - 0.116	0.081 - 0.125	0.000
ADH5	TRG	1.0	0.243	0.161 - 0.367	0.160 - 0.369	0.356
ADH8A	TRG	0.92	0.070	0.065 - 0.075	0.062 - 0.078	0.000
ADH8B	TRG	0.91	2.159	2.117 - 2.202	2.106 - 2.214	0.642
RALDH2	TRG	0.97	32.700	20.340 - 52.570	20.285 - 52.714	0.357
RARAA	TRG	0.94	0.876	0.787 - 0.975	0.770 - 0.996	1.000
RARAB	TRG	1.0	0.078	0.065 - 0.094	0.062 - 0.098	0.073
RARG	TRG	0.92	191.829	64.676 - 588.817	55.037 - 675.100	0.213
CYP26A1	TRG	0.95	0.101	0.094 - 0.109	0.092 - 0.112	0.073
CYP26B1	TRG	0.93	10.820	6.231 - 22.081	4.260 - 28.822	0.355

Legend:
P(H1) - Probability of alternate hypothesis that difference between sample and control groups is due only to chance.
TRG - Target
REF - Reference

A

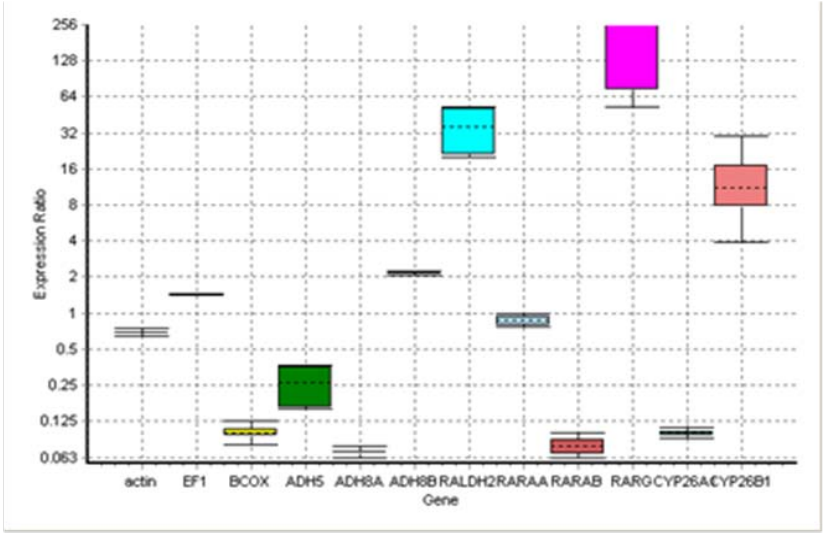

B

Figure 3-2. Relative Expression Software Tool (REST) data comparing the 24 hpf embryo time point to the 5 hpf embryo time point, and normalizing to two endogenous controls, actin and EF1α. A) The output of REST shows which genes are target, and which are reference. Reaction efficiency of 1.0 equals 100% amplification. B) Whisker-box plot of the results from table A shows a dotted line at the median, and skewed whisker or box size based on expression data variability.

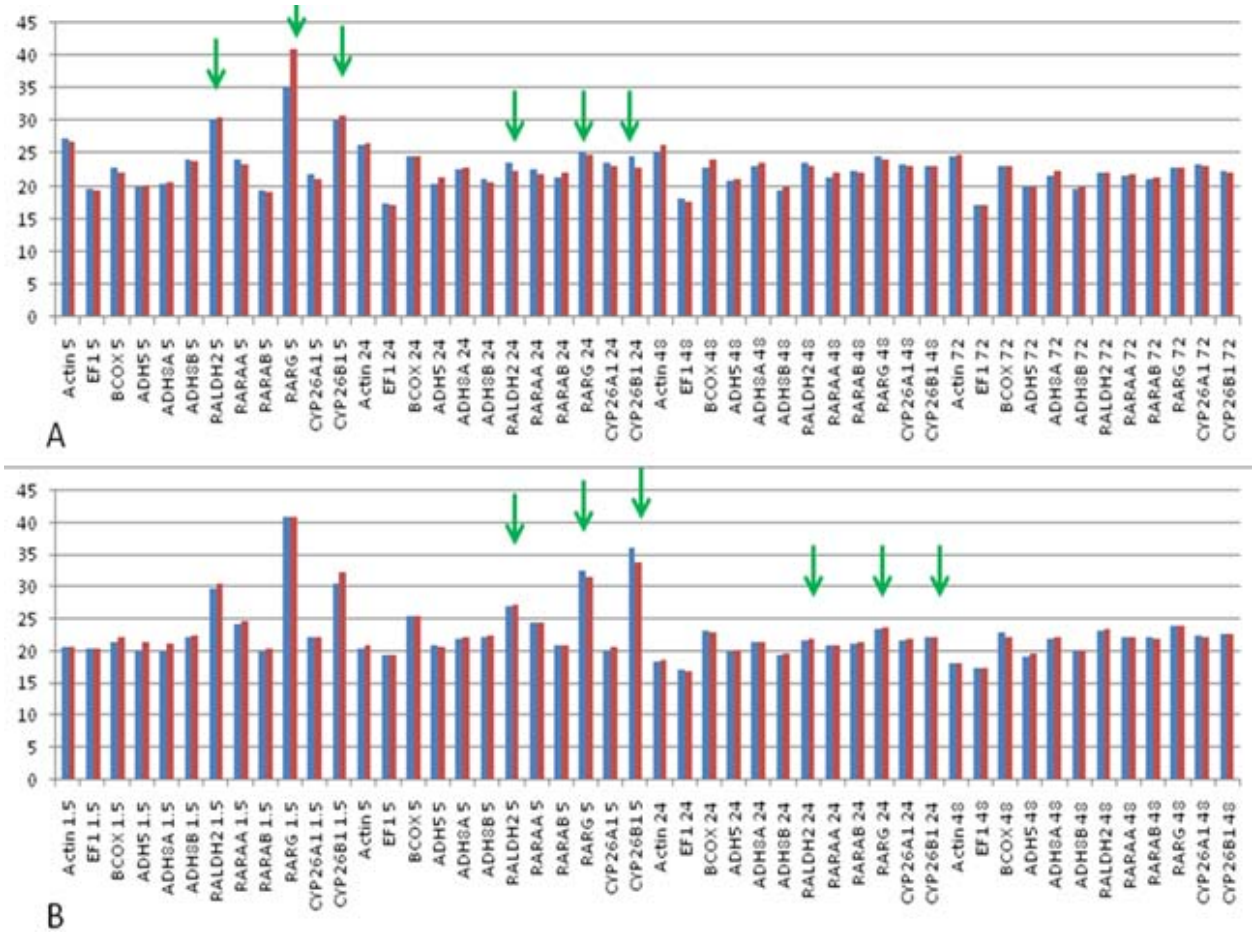

Figure 3-3. Excel graph of C_t's from duplicate real-time PCR assays performed on embryo RNA from different biological sample sets. A) Blue bars are the average of duplicate C_t's at each time point 5, 24, 48 and 72 hpf. Red bars are a duplicate of that assay. Green arrows indicate that RALDH2 5hpf, RARG 5hpf and CYP26B1 5 hpf visually have the greatest C_t value difference from actin and EF1α, the endogenous controls. B) Real-time PCR was repeated twice as in A with a biological replicate sample set of embryos from 1.5, 5, 24 and 48 hpf. The same three genes are displaying the greatest variability from the C_t values of the endogenous controls.

	RALDH2	RARG	CYP26B1
5 hpf	24 ± 6	1524 ± 206	82 ± 34
	11 ± 2	1500 ± 223	42 ± 3
	26 ± 5	1657 ± 361	35 ± 4
24 hpf	1882 ± 97	2770 ± 241	167 ± 10
	1740 ± 41	3286 ± 116	135 ± 15
	1899 ± 28	4845 ± 841	442 ± 30

A

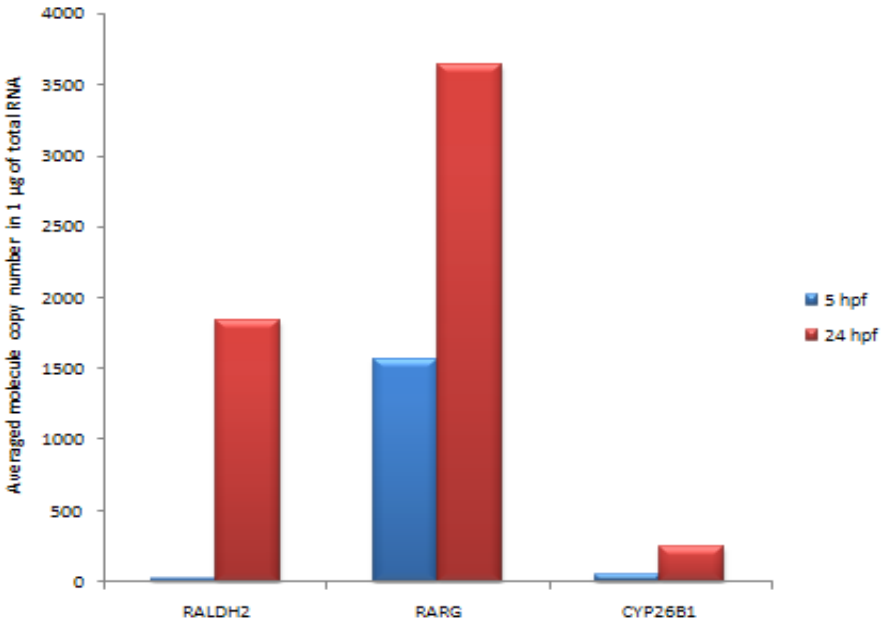

B

Figure 3-4. Representative results of averaged molecule copy number values from absolute quantification real-time PCR. A) Table of copy numbers representing the significant fold changes in gene expression from triplicate runs with standard deviation determination. B) Graph of molecule copy numbers in A demonstrating fold changes in gene expression of 100 for RALDH2, 2 for RARG and 3 for CYP26B1.

Probe Sequences for Northern Blotting

RALDH2- 115 bp

gagacagtgcttaccttgctaccctggagtctctggacagcggcaaacctttcctcccctgcttctttgtggaccttcaggggatcattaaa
acatttcgatattacgctggatgg

RARG- 88 bp

ggtgttgttattgttgttttggtgacgagaggcaatcggaggcgggtgggtgaccgggacgcagcatgttcgactgtatggaggctctg

CYP26B1- 181 bp

ttgttcagcaccttccaggagtttgtggagaacgtcttcagtcttcccatcgacctgccatttagtggttacagaaagggtattcgagcaag
agactcactccaaaaaagcatagagaaagccatcagagagaaaccactccacacacaggggaaagattacactgatgctcttgatgtg
ct

EF1α- 161 bp

tcaagaagatcggctacaaccctgccagtgttgccttcgtcccaatttcaggatggcacggtgacaacatgctggaggccagctcaaaca
tgggctggttcaagggatggaagattgagcgcaaggagggtaatgctagcggtactactcttcttgatgccc

Figure 3-5. The SYBR® Green amplified regions which were biotin labeled and used as probes to total RNA Northern blot.

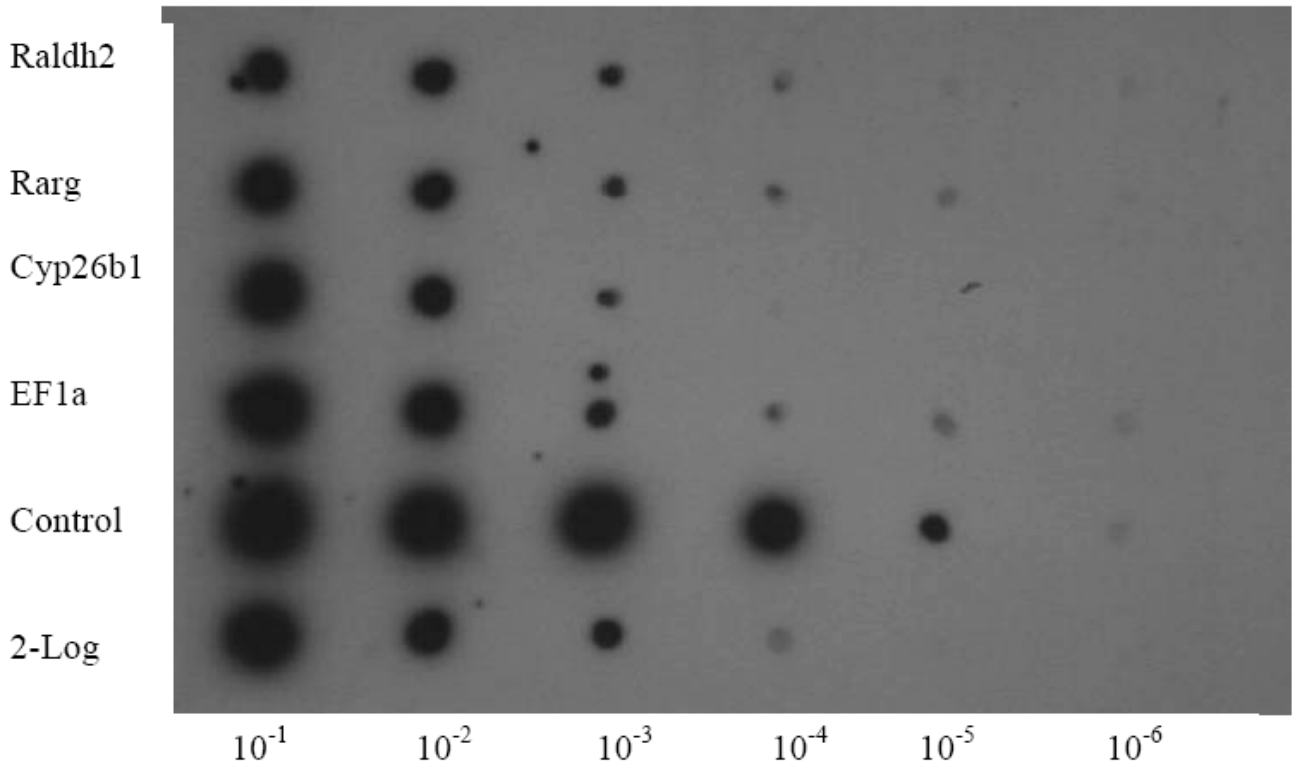

Figure 3-6. Dot blot of Northern blot probes to confirm adequate incorporation of biotinylated d-ATP. This autoradiograph shows that all probes are visible between (1 ng/µL) of the 2-Log DNA Ladder and (50 fg/ µL) of the lambda control and according to kit protocol are considered to have sufficient activity for use. The concentration of the probe as estimated by amount of starting material and length of reaction time is approximately 20 ng/µl.

RALDH2: $\frac{13655 \text{ molecules}}{1 \text{ µl}} \times \frac{1 \text{ mole molecules}}{6.023 \times 10^{23} \text{ molecules}} = \frac{2.27 \times 10^{-20} \text{ moles of molecules}}{1 \text{ µl}}$

$\times \frac{2244 \text{ mole bases}}{1 \text{ mole molecules}} = \frac{5.09 \times 10^{-17} \text{ mole of bases}}{1 \text{ µl}}$

$\times \frac{330 \text{ grams}}{1 \text{ mole bases}} = \frac{1.68 \times 10^{-14} \text{ grams}}{1 \text{ µl}}$

$\times \frac{10^{12} \text{ pg}}{1 \text{ gram}} = \frac{0.016 \text{ pg of target}}{1 \text{ µl RNA}}$

0.016 pg target x 20 µl RNA loaded = 0.32 pg total target

Summary of Amount of Target on the Northern Blot

RALDH2	0.32 pg
RARG	1.06 pg
CYP26B1	0.03 pg
EF1α	5.07 pg

Figure 3-7. Determination of amount of target RNA available for biotinylated cDNA probe. Based on 90 ng of total RNA as template per µl for each gene of interest the amount of message is calculated based on the molecule number derived from TaqMan® absolute quantification. According to Current Protocols, about 1 pg can be detected of target DNA on Southern blots using chemiluminescent detection (40). It is assumed that DNA probe hybridized to RNA is similar or slightly higher due to the stronger binding affinity between DNA and RNA.

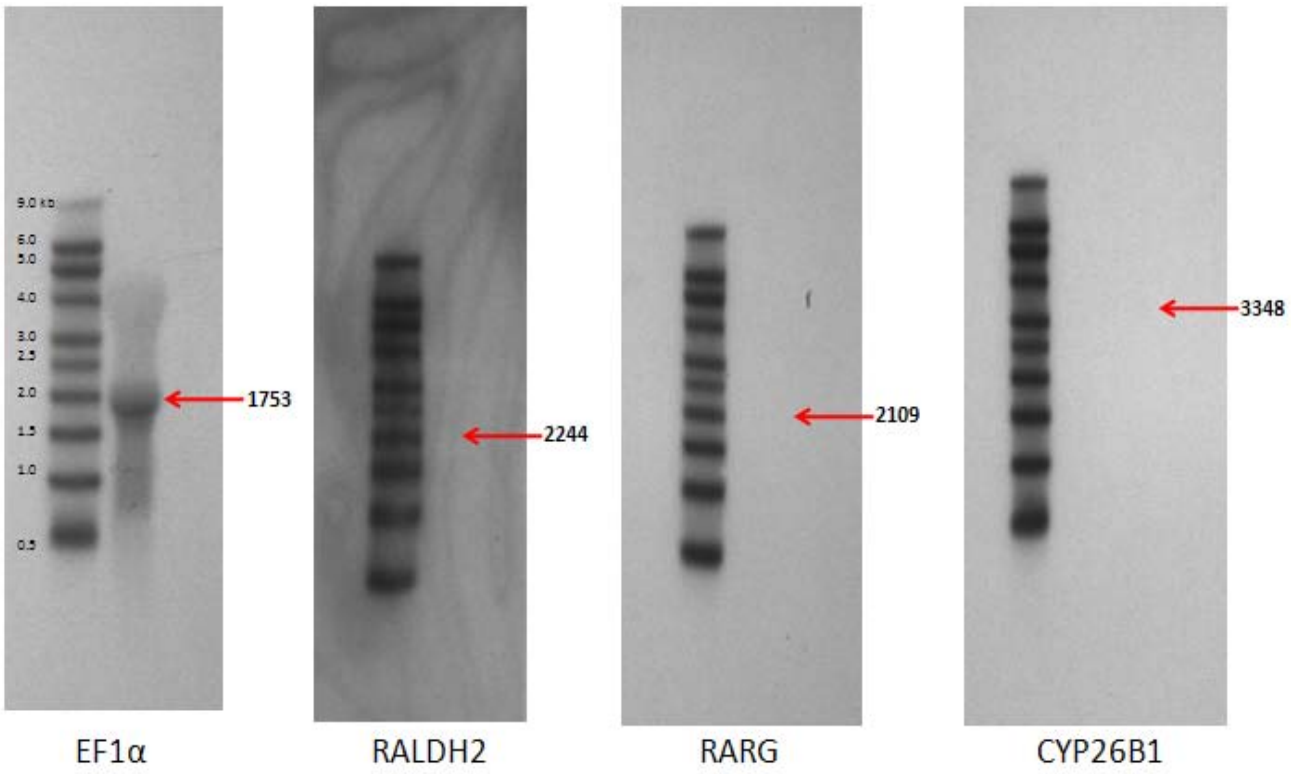

Figure 3-8. Northern blot analysis, each with 10 µg of total RNA. As predicted by the calculations in figure 3-8, only EF1α has enough target message to be detected by this method. The expected band locations for RALDH2, RARG and CYP26B1 are indicated.

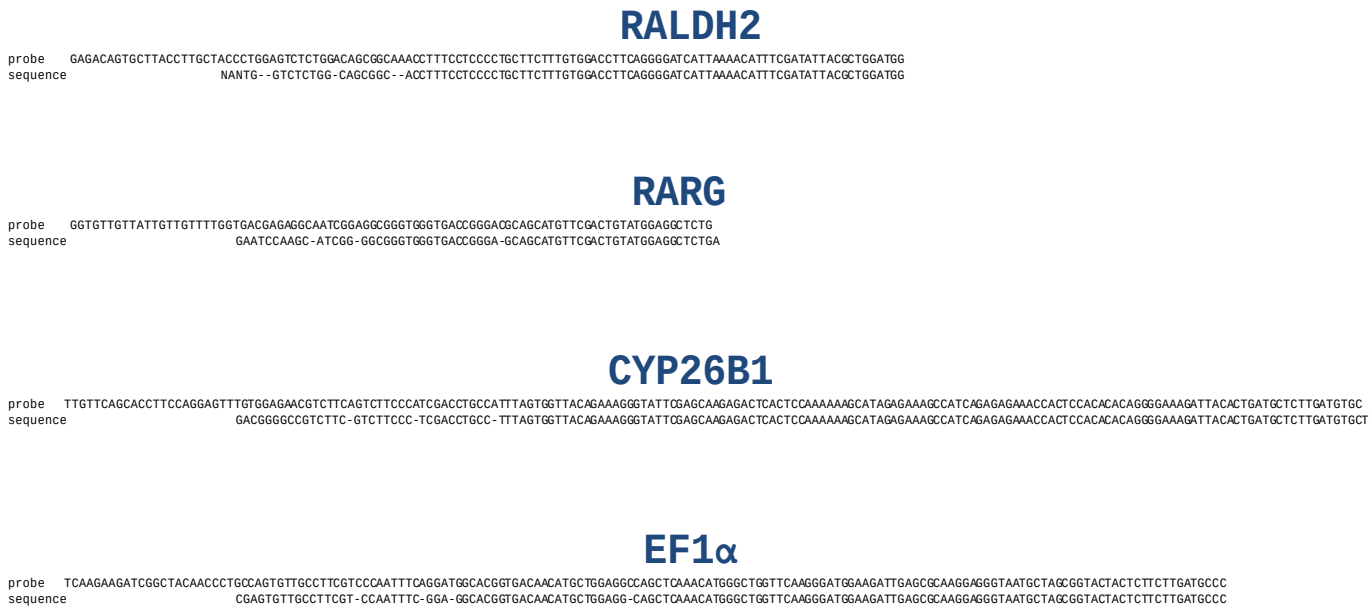

Figure 3-9. Amplified product was sequenced using the forward primer. Aliquots from SYBR® Green amplified products were submitted to the DNA Sequencing Core Laboratory and the results were aligned with the predicted sequences that were determined during primer design. The close match confirms accuracy and specificity of amplification during the real-time PCR assay.

CHAPTER 4
REAL-TIME PCR TRAINING

Course Information

As the Coordinator for the ICBR Education and Training Core Laboratory, I am responsible for the curriculum in a course taught twice yearly titled Protein Chemistry and Molecular Cloning. The class participants are faculty, staff and graduate students who desire hands-on training in common molecular techniques in order to enhance their own research. This 3 week course runs from 8:30 AM to 5 PM, Monday through Friday and seats between 30 and 60 students. Each student is provided with his own bench area equipped with basic equipment standard to a modern molecular biology research laboratory. All reagents necessary for a particular wet lab experiment are prepared by our staff and provided to students in labeled tubes.

The content starts with Protein techniques with the expression of human carbonic anhydrase II (hCAII) in *E. coli.* The protein is isolated, purified, de-salted, concentrated and quantified. Enzyme activity is assayed and then the proteomics techniques 2Dgel and Mass Spectrometry are used for further characterization and validation. The second part of the course moves into molecular cloning techniques with musculus CAII (mCAII). RNA and genomic DNA are isolated from mouse tissue. Reverse transcription and PCR optimization and amplification lead into cloning into vector for transformation into *E. coli.* Southern blotting with non-radioactive probe labeling and a concurrent bioinformatics project round out the course (Figure 4-1). Because real-time PCR is becoming a highly used technique for the characterization of message due to its speed and affordability, it would an important and useful addition to the course.

Training Exercise Development

The challenge with converting any wet lab bench procedure to a classroom environment is that timing, equipment availability, reagent cost, lecture content, and room dynamics all must come together and work cohesively. It also must fit with the other wet lab protocols so that the overall theme of CAII is conserved. Based on these parameters the real-time PCR hands-on training experiment using SYBR® Green was added to the curriculum beginning in July 2008. Total RNA from a variety of mouse tissues was provided to the students. Using primers for glyceraldehyde-3 phosphate dehydrogenase (GAPDH) and mCAII the students compared the relative expression of the normalized samples as a class using the REST program (Figure 4-2). The experiment was well received by the students as evidenced by several of the course evaluation comments: “I thought Exp 20 was very useful. A lot of people talk about RT-PCR but I had no experience with it, now I do.” and “The real-µtime PCR lecture was great.” This experiment will become a permanent addition to the course and undergo further revisions and improvements as feedback from course participants dictates. (Appendix)

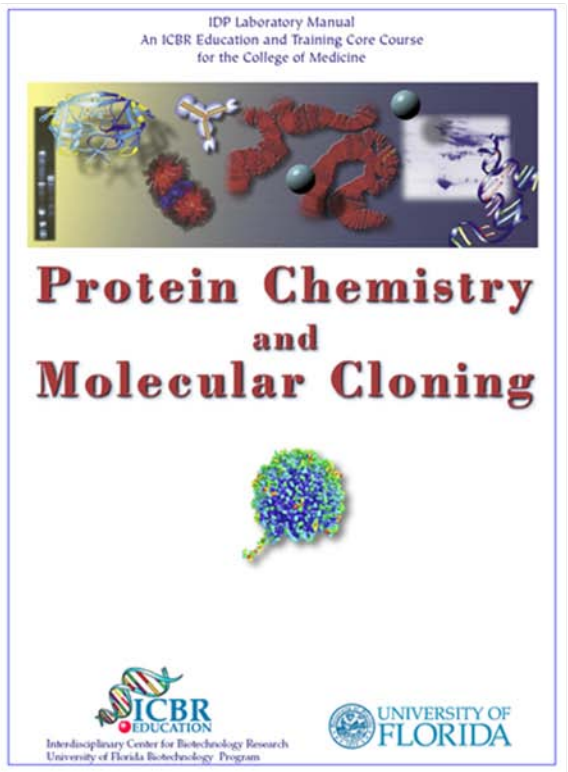

TABLE OF CONTENTS
IDP Laboratory Manual
August 19- September 3, 2008

Figure 4-1. Protein Chemistry and Molecular Cloning course at the University of Florida. As Coordinator for the ICBR Education and Training Core Laboratory, I am responsible for the content of the Protein Chemistry and Molecular Cloning workshop which is taught twice annually. This three week long, eight hours per day, laboratory course covers a wide range of topics which up until this year did not include real-time PCR. As instrumentation for real time PCR becomes more accessible the technique is seeing greater use and basic training in graduate level courses has become necessary.

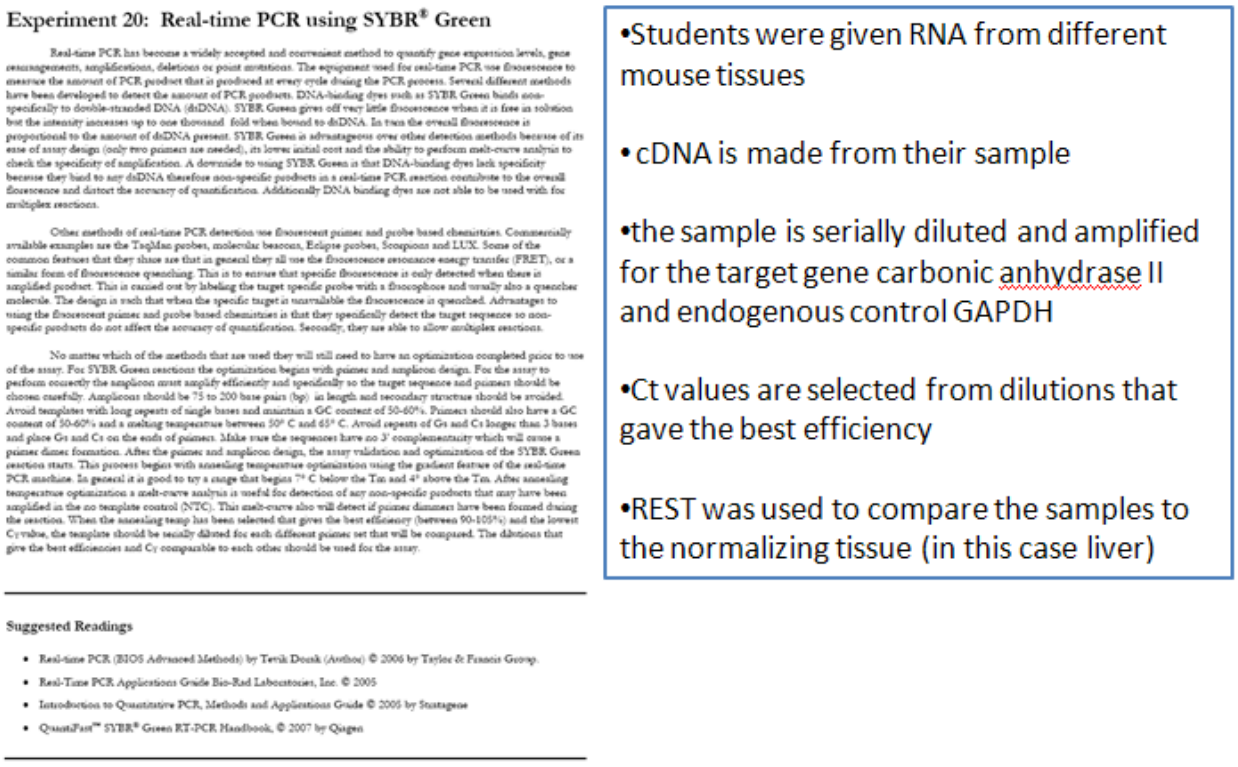

Experiment 20: Real-time PCR using SYBR® Green

Real-time PCR has become a widely accepted and convenient method to quantify gene expression levels, gene rearrangements, amplifications, deletions or point mutations. The equipment used for real-time PCR use fluorescence to measure the amount of PCR product that is produced at every cycle during the PCR process. Several different methods have been developed to detect the amount of PCR products. DNA-binding dyes such as SYBR Green bind to non-specifically to double-stranded DNA (dsDNA). SYBR Green gives off very little fluorescence when it is free in solution but the intensity increases up to one thousand fold when bound to dsDNA. In turn the overall fluorescence is proportional to the amount of dsDNA present. SYBR Green is advantageous over other detection methods because of its ease of assay design (only two primers are needed), its lower initial cost and the ability to perform melt-curve analysis to check the specificity of amplification. A downside to using SYBR Green is that DNA-binding dyes lack specificity because they bind to any dsDNA therefore non-specific products in a real-time PCR reaction contribute to the overall fluorescence and distort the accuracy of quantification. Additionally DNA binding dyes are not able to be used with for multiplex reactions.

Other methods of real-time PCR detection use fluorescent primer and probe based chemistries. Commercially available examples are the TaqMan probes, molecular beacons, Eclipse probes, Scorpions and LUX. Some of the common features that they share are that in general they all use the fluorescence resonance energy transfer (FRET), or a similar form of fluorescence quenching. This is to ensure that specific fluorescence is only detected when there is amplified product. This is caused out by labeling the target specific probe with a fluorophore and usually also a quencher molecule. The design is such that when the specific target is unavailable the fluorescence is quenched. Advantages to using the fluorescent primer and probe based chemistries is that they specifically detect the target sequence so non-specific products do not affect the accuracy of quantification. Secondly, they are able to allow multiplex reactions.

No matter which of the methods that are used they will still need to have an optimization completed prior to use of the assay. For SYBR Green reactions the optimization begins with primer and amplicon design. For the assay to perform correctly the amplicon must amplify efficiently and specifically so the target sequence and primers should be chosen carefully. Amplicons should be 75 to 200 base pairs (bp) in length and secondary structure should be avoided. Avoid templates with long repeats of single bases and maintain a GC content of 50-60%. Primers should also have a GC content of 50-60% and a melting temperature between 50° C and 65° C. Avoid repeats of Gs and Cs longer than 3 bases and place Gs and Cs on the ends of primers. Make sure the sequences have no 3' complementarity which will cause a primer dimer formation. After the primer and amplicon design, the assay validation and optimization of the SYBR Green reaction starts. This process begins with annealing temperature optimization using the gradient feature of the real-time PCR machine. In general it is good to try a range that begins 7° C below the Tm and 4° above the Tm. After annealing temperature optimization a melt-curve analysis is useful for detection of any non-specific products that may have been amplified in the no template control (NTC). This melt-curve also will detect if primer dimmers have been formed during the reaction. When the annealing temp has been selected that gives the best efficiency (between 90-105%) and the lowest Cy value, the template should be serially diluted for each different primer set that will be compared. The dilutions that give the best efficiencies and Cy comparable to each other should be used for the assay.

Suggested Readings

- Real-time PCR (BIOS Advanced Methods) by Tevik Dorak (Author) © 2006 by Taylor & Francis Group.
- Real-Time PCR Applications Guide Bio-Rad Laboratories, Inc. © 2005
- Introduction to Quantitative PCR, Methods and Applications Guide © 2005 by Stratagene
- QuantiFast™ SYBR® Green RT-PCR Handbook, © 2007 by Qiagen

Figure 4-2. Hands-on real-time PCR training experiment. In order to fulfill the work requirements of my position at the ICBR Education and Training Core Laboratory while simultaneously completing the research in this thesis, the knowledge gained from this research was written to a hands-on training exercise in real-time PCR for graduate student level courses.

CHAPTER 5
DISCUSSION

The data resulting from the studies in this thesis indicate that real-time PCR can be used to quantify changes in mRNA expression during early development of zebrafish. This technique is able to detect and quantify the gene target with greater specificity and speed at a lower cost, with less time required to master technically compared to *in situ* hybridization. The validation and repetition of results confirm that real-time PCR is a reliable alternative to the more expensive and time consuming *in situ* hybridization. Tissue distribution and cellular localization however are not determined by real-time PCR. For example, it would not be able to demonstrate that CYP26B1 is expressed in diencephalon, eyes, midbrain hindbrain boundary and cerebellum of the 24 hpf embryo.

The original screening panel of all twelve primer sets comparing adult fish with 5 hpf, 24 hpf and 48 hpf embryos provided the initial information that there is sufficient change in gene expression at these time points to pursue further studies in this system. To characterize better the early results a second set of samples with overlapping time points was isolated and assayed with the same primer sets and SYBR® Green real-time PCR. The results of both sample sets assayed multiple times resulted in a visual Excel graph that shows the greatest fold change in expression during the early zebrafish development was in RALDH2, RARG and CYP26B1. The C_t values for both sets were also analyzed using the REST program which further confirmed the larger fold change in these three particular gene messages. The absolute quantification of the number of molecules in a sample was calculated using TaqMan® primers and probes with a standard curve. Accuracy was maximized by the correct placement of the threshold line. The standard curve to which unknown samples are compared to for quantification is defined as the line equation $y = mx + b$ where m is the slope and b is the y-intercept. Theoretically if there is perfect doubling of

the template at each cycle then the slope would be -3.32. The threshold line should be placed where the slope is close to this value. In addition, the r^2 value that indicates how close to the regression line the data points lie should be between 0.990 and 1. With these parameters met a two- fold change in copy number has a difference of one C_t value. Properly placed thresholds were set for all absolute quantification data. The EF1α was found to be in a great excess over the RALDH2, RARG and CYP26B1 which was to be expected. When the overall trends in the increase or decrease in expression between different time points is considered between the data from SYBR® Green assays and TaqMan® assays, it was found they correlated very well. Along with the quality of the data from the standard curve, this correlation gave a high level of confidence in being able to state if gene expression increases or decreases.

Since it is so profoundly important for retinoic acid to be delivered at the right amount, in the right place and at the right time, it would be essential for the developing organism to have the necessary enzymes and receptors to process vitamin A at an early stage. Changes in gene expression for RALDH2, RARG, and CYP26B1 at 5-24 hpf are consistent with the need for retinoic acid synthesis, utilization, and degradation following the mid-blastula transition (~3 hpf) to support the conversion of yolk vitamin A to retinoic acid, a key regulator of gene expression during development. Since RA regulates development by activating gene transcription, a cell will only respond to RA if there are receptors expressed to bind it. Because the concentration of RA must lie within an acceptable range or it could be teratogenic for the organism, mechanisms must be in place to remove the excess. RALDH2 converts vitamin A to the usable RA form, RARG binds RA, a necessary step for RA to affect gene regulation, and CYP26B1 as an RA inducible catabolic enzyme will presumably play a role in not allowing RA to reach teratogenic levels. It is

not surprising that these three key enzymes and receptors are changing dramatically in early zebrafish development because basic proper growth requires their expression and interaction.

The cDNA probe sequences used for Northern blotting were determined by where the real-time PCR primers annealed in the sequence provided by the accession number. Knowing the exact sequence was necessary to optimize the biotin labeling protocol. A small aliquot of the template that was used for the probe labeling was sent to the ICBR DNA sequencing facility and the results confirmed that the actual and predicted sequences do align well. It was also required information for the calculation of how much target message would be on the Northern blot based on the amount of total RNA that is loaded on the denaturing agarose gel. Based on the general knowledge that non-radioactive Northern blots would require a minimum of about a picogram of target to be detected, it was determined that EF1α would be the only message that would be able to be detected on Northerns with 10 µg of total RNA loaded. This calculation was confirmed by the results of the Northern blots. The only gel with a band detected was that of the EF1α and the band size was consistent with the information presented on NCBI via the accession number. Radioactively labeled probes used to be considered a more sensitive detection system but with today's new robust substrates such as CDP-Star, this is no longer the case as their results are quite similar. Another consideration for using non-radioactively labeled probes is that the facility is used for teaching and training and it is not feasible to expose untrained people to radioisotopes in the classroom.

The knowledge gained during the research of this thesis provided a very positive addition to a training course that has been taught twice annually for the last 15 years at the University of Florida. The technique of real-time PCR as demonstrated here has proven to be a fast, specific and cost effective method to characterize gene expression. It should be included in a course that

teaches many basic hands-on protein chemistry and molecular cloning techniques and it was successfully integrated this year. Opinion comments were included in the results section indicating that the students acknowledge that they find it important to have exposure to this technique. In future iterations of the course a pre and post knowledge and opinion assessment would help better to measure the level of benefit to the student and give suggestions for improvements. Additionally, the experiment could be upgraded to include standard curve construction and absolute quantification with TaqMan® primer and probes.

Finally, given the ubiquity of the retinoic acid pathway, the genes examined here could be used as biomarkers to examine the effects of anthropogenic or naturally occurring biological toxins on early vertebrate development. Combined with the speed and accuracy of real-time PCR this system could potentially have very useful applications.

APPENDIX
ICBR TRAINING EXERCISE

Experiment 20: Real-time PCR using SYBR® Green

Real-time PCR has become a widely accepted and convenient method to quantify gene expression levels, gene rearrangements, amplifications, deletions or point mutations. The equipment used for real-time PCR use fluorescence to measure the amount of PCR product that is produced at every cycle during the PCR process. Several different methods have been developed to detect the amount of PCR products. DNA-binding dyes such as SYBR® Green binds non-specifically to double-stranded DNA (dsDNA). SYBR® Green gives off very little fluorescence when it is free in solution but the intensity increases up to one thousand fold when bound to dsDNA. In turn the overall fluorescence is proportional to the amount of dsDNA present. SYBR® Green is advantageous over other detection methods because of its ease of assay design (only two primers are needed), its lower initial cost and the ability to perform melt-curve analysis to check the specificity of amplification. A downside to using SYBR® Green is that DNA-binding dyes lack specificity because they bind to any dsDNA therefore non-specific products in a real-time PCR reaction contribute to the overall florescence and distort the accuracy of quantification. Additionally DNA binding dyes are not able to be used with for multiplex reactions.

Other methods of real-time PCR detection use fluorescent primer and probe based chemistries. Commercially available examples are the TaqMan® probes, molecular beacons, Eclipse probes, Scorpions and LUX. Some of the common features that they share are that in general they all use the fluorescence resonance energy transfer (FRET), or a similar form of fluorescence quenching. This is to ensure that specific fluorescence is only detected when there is amplified product. This is carried out by labeling the target specific probe with a fluorophore and usually also a quencher molecule. The design is such that when the specific target is unavailable the fluorescence is quenched. Advantages to using the fluorescent primer and probe based chemistries is that they specifically detect the target sequence so non-specific products do not affect the accuracy of quantification. Secondly, they are able to allow multiplex reactions.

No matter which of the methods that are used they will still need to have an optimization completed prior to use of the assay. For SYBR® Green reactions the optimization begins with primer and amplicon design. For the assay to perform correctly the amplicon must amplify efficiently and specifically so the target sequence and primers should be chosen carefully. Amplicons should be 75 to 200 base pairs (bp) in length and secondary structure should be avoided. Avoid templates with long repeats of single bases and maintain a GC content of 50-60%. Primers should also have a GC content of 50-60% and a melting temperature between 50° C and 65° C. Avoid repeats of Gs and Cs longer than 3 bases and place Gs and Cs on the ends of primers. Make sure the sequences have no 3' complementarity which will cause a primer dimer formation. After the primer and amplicon design, the assay validation and optimization of the SYBR® Green reaction starts. This process begins with annealing temperature optimization using the gradient feature of the real-time PCR machine. In general it is good to try a range that begins 7° C below the Tm and 4° above the Tm. After annealing temperature optimization a melt-curve analysis is useful for detection of any non-specific products that may have been amplified in the no template control (NTC). This melt-curve also will detect if primer dimers have been formed

during the reaction. When the annealing temp has been selected that gives the best efficiency (between 90-105%) and the lowest C_t value, the template should be serially diluted for each different primer set that will be compared. The dilutions that give the best efficiencies and C_t comparable to each other should be used for the assay.

Suggested Readings

- Real-time PCR (BIOS Advanced Methods) by Tevik Dorak (Author) © 2006 by Taylor & Francis Group.
- Real-Time PCR Applications Guide Bio-Rad Laboratories, Inc. © 2005
- Introduction to Quantitative PCR, Methods and Applications Guide © 2005 by Stratagene
- QuantiFast™ SYBR® Green RT-PCR Handbook, © 2007 by Qiagen

Part A: Experimental Plan

Always **wear gloves** and maintain all reagent solutions on ice, unless indicated otherwise.

In this experiment, you will be given total RNA from a mouse tissue and you will create cDNA which will be used to set up real-time PCR reactions for carbonic andhydrase and our normalizer GAPDH (glyceraldehyde 3-phosphate dehydrogenase). Different groups will receive different tissues and we will compare the relative amount of normalized carbonic anhydrase expression among the tissues. The liver CA and GAPDH will serve as our overall basis for relative expression. Due to time constraints the primers have been optimized for you and your samples will have only a limited number of dilutions. Normally a NTC control is included with your samples which are run in at least duplicate. Due to limited machine availability there will be no NTC and and the samples will be set up only one time at 4 different dilutions for each primer set.

Note: Continue to observe the same guidelines for RNA isolation (i.e., RNase-free handling) during the cDNA synthesis step.

1. Label a PCR tube with your group number and add reagents to the tube as written in the chart below:

cDNA reaction tubes

Reagent	**cDNA for real-time PCR (µL)**	**Final conc.**
Water	13	----
5X iScript reverse transcription	4	1X
iScript reverse transcriptase	1	----
Mouse tissue RNA (0.5 ug/µl)	2	1 ug total
Total reaction	**20**	

2. Place your samples on ice until everyone in the class is done, then bring samples to the thermocycler.

3. Transfer tubes to the thermocycler that has been programmed using the following parameters:

    5 minutes at 25° C
    30 minutes at 42° C
    5 minutes at 85° C
    Hold at 14° C

4. When the cDNA reaction is complete, retrieve the tube from the PCR machine. Transfer the entire 20 µl of cDNA to a new 1.5 mL tube and add 180 µl of water to the cDNA for a 1:10 dilution.

5. Serially dilute the cDNA 10 fold, 3 additional times each with 2 µl of cDNA and 18 µl of water.

6. Place the white PCR tube strip into a rack with the "A" at the top, label the "A" with your group number.

7. Prepare 2 Master mixes each one at 4.5 X for both the carbonic anhydrase and the GAPDH according to the chart below. Make sure to use the appropriate primers for the Master mix.

Reagent	**Amount per sample (µl)**	**Amount per 4.5 samples (µl)**	**Final conc.**
iQ SYBR® Green Supermix	12.5	56.25	1X
Primer 1 (10 µM)	0.5	2.25	200 nM
Primer 2 (10 µM)	0.5	2.25	200 nM
Water	10.5	47.25	----
cDNA template	1	----	Varies
TOTAL VOLUME/SAMPLE	25 µL	----	---

8. Starting at the top with the "A" add 24 µl to well numbers 1 through 4 of the carbonic anhydrase master mix. Add 24 µl of the GAPDH master mix to wells 5 through 8.

9. Add 1 µl of the different dilutions of cDNA to the appropriate well according to the chart below:

CA 10 fold
CA 100 fold
CA 1000 fold
CA 10000 fold
GAPDH 10 fold
GAPDH 100 fold
GAPDH 1000 fold
GAPDH 10000 fold

10. Place your samples on ice until everyone in the class is done, then bring samples to the thermocycler.

11. Transfer tubes to the thermocycler that has been programmed using the following parameters:

    95° C for 3 minutes
    95° C for 10 seconds
    57° C for 1 minute
    Plate read
    GOTO step 2, 39 times
    End

Exercise : Use REST to analyze the real-time data.

The following information is from this web site http://www.gene-quantification.de/

REST 2005 is a new standalone software tool to estimate up and down-regulation for gene expression studies. The software addresses issues surrounding the measurement of uncertainty for expression ratios, by using randomisation and bootstrapping techniques. By increasing the number of iterations from 2,000 to 50,000 in this version hypothesis tests achieve a level of consistency on par with traditional statistical tests. New confidence intervals for expression levels also allow scientists to measure not only the statistical significance of deviations, but also their likely magnitude, even in the presence of outliers. Graphical output of the data via a whisker box-plots provide a visual representation of variation for each gene that highlights potential issues such as distribution skew.

1. Double click the REST icon on the desktop to open the application.
2. Click on the tab labeled Setup.
3. Click the Add button and enter the tissue LIVER, click the reference box and enter the reaction efficiency as 1
4. In the sample box enter the C_t value for your LIVER CA that has an efficiency that is close to 100%, in the control box enter the C_t value for the LIVER GAPDH that has an efficiency that is close to 100%. Nothing is entered for std. because we do not have a standard curve on the run.
5. Click Add and repeat the process for CA and GAPDH from different tissues but do not click the reference box.
6. Check the Results Tab and the Graph tab. You have normalized your data and compared relative expression of your tissue's CA to that of the liver CA.
7. Enter the data from other tissue samples in the class and look at the relative expression.

LIST OF REFERENCES

1. Dietary Supplement Fact Sheet: Vitamin A and Carotenoids. (6/22/2005). http://ods.od.nih.gov/factsheets/vitamina.asp 11/20/2008

2. Saari, J.C. Biochemistry of visual pigment regeneration: the Friedenwald lecture. *Invest Ophthalmol Vis Sci* **41**, 337-348 (2000).

3. Immunization Vitamin A. (2008). http://www.unicef.org/immunization/23245_vitamina.html 11/20/08

4. Underwood, B.A. & Arthur, P. The contribution of vitamin A to public health. *Faseb J* **10**, 1040-1048 (1996).

5. Duester, G. Families of retinoid dehydrogenases regulating vitamin A function: production of visual pigment and retinoic acid. *Eur J Biochem* **267**, 4315-4324 (2000).

6. Ross, A.C. Retinoid production and catabolism: role of diet in regulating retinol esterification and retinoic Acid oxidation. *J Nutr* **133**, 291S-296S (2003).

7. Ma, Y., Chen, Q. & Ross, A.C. Retinoic acid and polyriboinosinic:polyribocytidylic acid stimulate robust anti-tetanus antibody production while differentially regulating type 1/type 2 cytokines and lymphocyte populations. *J Immunol* **174**, 7961-7969 (2005).

8. DeCicco, K.L., Youngdahl, J.D. & Ross, A.C. All-trans-retinoic acid and polyriboinosinic : polyribocytidylic acid in combination potentiate specific antibody production and cell-mediated immunity. *Immunology* **104**, 341-348 (2001).

9. Mora, J.R. & von Andrian, U.H. Retinoic acid: an educational "vitamin elixir" for gut-seeking T cells. *Immunity* **21**, 458-460 (2004). Mora, J.R. & von Andrian, U.H. Retinoic acid: an educational "vitamin elixir" for gut-seeking T cells. *Immunity* **21**, 458-460 (2004).

10. Hale, B. Combination Treatment Enhances Tetanus Vaccination. (9/12/2008). http://www.eurekalert.org/pub_releases/2005-09/ps-cte091205.php 11/20/08

11. Douer, D. & Koeffler, H.P. Retinoic acid enhances growth of human early erythroid progenitor cells in vitro. *J Clin Invest* **69**, 1039-1041 (1982).

12. Ostrom, M. et al. Retinoic acid promotes the generation of pancreatic endocrine progenitor cells and their further differentiation into beta-cells. *PLoS ONE* **3**, e2841 (2008).

13. O'Shea, F.D. et al. Retinol (vitamin A) and retinol-binding protein levels are decreased in ankylosing spondylitis: clinical and genetic analysis. *J Rheumatol* **34**, 2457-2459 (2007).

14. Christian, P. & West, K.P., Jr. Interactions between zinc and vitamin A: an update. *Am J Clin Nutr* **68**, 435S-441S (1998).

15. Jang, J.T., Green, J.B., Beard, J.L. & Green, M.H. Kinetic analysis shows that iron deficiency decreases liver vitamin A mobilization in rats. *J Nutr* **130**, 1291-1296 (2000).

16. Rosales, F.J. et al. Iron deficiency in young rats alters the distribution of vitamin A between plasma and liver and between hepatic retinol and retinyl esters. *J Nutr* **129**, 1223-1228 (1999).

17. Maden, M. The role of retinoic acid in embryonic and post-embryonic development. *Proc Nutr Soc* **59**, 65-73 (2000).

18. Shenefelt, R.E. Morphogenesis of malformations in hamsters caused by retinoic acid: relation to dose and stage at treatment. *Teratology* **5**, 103-118 (1972).

19. Marletaz, F., Holland, L.Z., Laudet, V. & Schubert, M. Retinoic acid signaling and the evolution of chordates. *Int J Biol Sci* **2**, 38-47 (2006).

20. Gene Cards ADH5 Gene. (2008). http://www.genecards.org/cgi-bin/carddisp.pl?gene=ADH5 11/21/08

21. Reimers, M.J., Hahn, M.E. & Tanguay, R.L. Two zebrafish alcohol dehydrogenases share common ancestry with mammalian class I, II, IV, and V alcohol dehydrogenase genes but have distinct functional characteristics. *J Biol Chem* **279**, 38303-38312 (2004).

22. Nadauld, L.D., Shelton, D.N., Chidester, S., Yost, H.J. & Jones, D.A. The zebrafish retinol dehydrogenase, rdh1l, is essential for intestinal development and is regulated by the tumor suppressor adenomatous polyposis coli. *J Biol Chem* **280**, 30490-30495 (2005).

23. Niederreither, K., Vermot, J., Fraulob, V., Chambon, P. & Dolle, P. Retinaldehyde dehydrogenase 2 (RALDH2)- independent patterns of retinoic acid synthesis in the mouse embryo. *Proc Natl Acad Sci U S A* **99**, 16111-16116 (2002).

24. Ribes, V., Wang, Z., Dolle, P. & Niederreither, K. Retinaldehyde dehydrogenase 2 (RALDH2)-mediated retinoic acid synthesis regulates early mouse embryonic forebrain development by controlling FGF and sonic hedgehog signaling. *Development* **133**, 351-361 (2006).

25. Ray, W.J., Bain, G., Yao, M. & Gottlieb, D.I. CYP26, a novel mammalian cytochrome P450, is induced by retinoic acid and defines a new family. *J Biol Chem* **272**, 18702-18708 (1997).

26. Taimi, M. et al. A novel human cytochrome P450, CYP26C1, involved in metabolism of 9-cis and all-trans isomers of retinoic acid. *J Biol Chem* **279**, 77-85 (2004).

27. Dunlap, L. Biomarker Assay Use Increases. *Genetic Engineering & Biotechnology News* **28**, 56-60 (2008).

28. Knight, J. Zebrafish K-12. http://www.neuro.uoregon.edu/k12/zfk12.html 11/20/08

29. Dahm, C.N.-V.a.R. Zebrafish A Practical Approach. 219-236 (2002).

30. Saari, J.C. The sights along route 65. *Nat Genet* **29**, 8-9 (2001).

31. Kimmel, C.B., Ballard, W.W., Kimmel, S.R., Ullmann, B. & Schilling, T.F. Stages of embryonic development of the zebrafish. *Dev Dyn* **203**, 253-310 (1995).

32. Odilo Mueller, S.L., Andreas Schroeder RNA Integrity Number (RIN) Standardization of RNA Quality Control. (2004).

33. Hwang, S.P., Tsou, M.F., Lin, Y.C. & Liu, C.H. The zebrafish BMP4 gene: sequence analysis and expression pattern during embryonic development. *DNA Cell Biol* **16**, 1003-1011 (1997).

34. Montgomery, S.M. In situ Hybridization. (2002). http://osiris.rutgers.edu/~smm/in_situ_hybridization.htm 11/20/08

35. Biedermann, K. et al. Comparison of real-time PCR signal-amplified in situ hybridization and conventional PCR for detection and quantification of human papillomavirus in archival cervical cancer tissue. *J Clin Microbiol* **42**, 3758-3765 (2004).

36. Wingert, R.A. et al. The cdx genes and retinoic acid control the positioning and segmentation of the zebrafish pronephros. *PLoS Genet* **3**, 1922-1938 (2007).

37. Thisse, B., Thisse, Christine, Expression from: Unexpected Novel Relational Links Uncovered by Extensive Developmental Profiling of Nuclear Receptor Expression (2008). http://zfin.org/cgi-bin/webdriver?MIval=aa-pubview2.apg&OID=ZDB-PUB-080220-1 11/21/08

38. Zhao, Q., Dobbs-McAuliffe, B. & Linney, E. Expression of cyp26b1 during zebrafish early development. *Gene Expr Patterns* **5**, 363-369 (2005).

39. Pfaffl, M.W. REST 2005. (2005). http://www.gene-quantification.de/ 11/21/08

40. Joeseph Sambrook, D.W.R. Molecular Cloning A Laboratory Manual. **2**, 9.79 (2001).

41. Feinberg, A.P. & Vogelstein, B. A technique for radiolabeling DNA restriction endonuclease fragments to high specific activity. *Anal Biochem* **132**, 6-13 (1983).

BIOGRAPHICAL SKETCH

Sharon Norton was born in Abington, Pennsylvania and resided in Devon, Pennsylvania, on the Main Line outside of Philadelphia in Tredyffrin Township. Sharon moved to Vero Beach, Florida, in 1980, where she and her father lived together on their twenty-eight foot Sabre sailboat while Sharon attended Vero Beach Senior High School. In 1985 Sharon moved to Gainesville, Florida to attend Santa Fe Community College and eventually earn an Associate of Science degree. After spending time in the workforce in a variety of positions including Blood Bank Laboratory Assistant and Tropical Fish Store Attendant, she enrolled in the University of Florida and in 1994 earned a Bachelor of Science degree majoring in microbiology and cell science with a minor in chemistry.

Sharon worked as a Research Technician at the University of Florida for two years and then left for a position in Alachua, Florida at CuraGen Corporation as a Laboratory Manager. In November of 1998, she returned to the University of Florida to work for the Interdisciplinary Center for Biotechnology Research as a Senior Biological Scientist. Sharon remains at the same job today and after two promotions now leads the Education and Training Core Laboratory as the Science Education Coordinator. In the spring semester of 2006 and while still employed full time, she enrolled in the College of Medicine master's Program at the University of Florida and under the guidance of her mentor, Dr. Peter McGuire, she received her M.S. from the University of Florida in the spring of 2009. Sharon has a six year old son, Nicholas, and a husband of ten years, Michael.